

# Máster en Física Avanzada

Especialidad teórica



## Trabajo Fin de Máster

---

Deviations from newtonian gravity in a  
two-branes model in 4+1 dimensions

Santiago González Marimón

Tutor : Andrea Donini

---

---

# Deviations from newtonian gravity in a two-branes model in 5 dimensions

Santiago Gonzlez Marimn      September 23, 2015

## Contents

<b>1</b>	<b>Introduction and motivation</b>	<b>4</b>
1.1	Experimental problems of the Standard Model . . . . .	4
1.2	The hierarchy problem . . . . .	5
1.3	Possible solutions to the hierarchy problem . . . . .	6
1.4	LED model . . . . .	6
1.5	Many-branes model . . . . .	7
<b>2</b>	<b>Gravity in presence of two or more branes</b>	<b>8</b>
2.1	Concept of brane . . . . .	8
2.2	R dependence on n . . . . .	9
2.3	Gravitational potential in five dimensions . . . . .	10
2.3.1	Corrections at big distances . . . . .	13
2.3.2	Corrections at small distances . . . . .	14
2.4	Force . . . . .	14
2.4.1	Corrections at big distances . . . . .	16
2.4.2	Corrections at small distances . . . . .	16
2.5	Bounds on R . . . . .	17
<b>3</b>	<b>Deviations from newtonian gravity: a <i>gedanken experiment</i></b>	<b>18</b>
3.1	Falling towards a dark matter particle . . . . .	19
3.2	Orbiting around a dark matter particle . . . . .	20
3.3	Results for orbital motion . . . . .	22
3.3.1	Period . . . . .	22
3.3.2	Eccentricity . . . . .	27
<b>4</b>	<b>Overview and open problems when facing DM</b>	<b>30</b>
4.1	Cosmic Microwave Background (CMB) . . . . .	30
4.2	Direct observation . . . . .	30
4.3	Indirect Observation . . . . .	31
4.4	Baryonic Acoustic Oscillations (BAO) . . . . .	32
4.5	Rotational curves and gravitational lensing . . . . .	33
<b>5</b>	<b>Conclusions</b>	<b>35</b>
<b>6</b>	<b>Appendix A: Conventions</b>	<b>36</b>
<b>7</b>	<b>Appendix B: Kaluza and Klein hypothesis (KK)</b>	<b>36</b>

---

## Abstract

In this brief work we propose a scenario that considers the existence of two, or many, parallel branes placed in a 4+1 dimensional bulk. This scenario has the main goal of explaining dark matter as Standard Model particles located in these parallel branes. The potential and effective force suffered by the particles are computed. A *gedanken experiment* for the most simple case is proposed: just one particle in each brane interacting via gravitation. Differences between this movement and that generated classically by Newton's square law are studied. Comments on direct and direct observation of dark matter particles, and other open problems, in our model are briefly discussed.

## Resumen

En este corto trabajo proponemos un escenario que consiste en dos, o mas, branas paralelas situadas en un espacio de 4+1 dimensiones. El principal objetivo de este escenario es explicar la materia oscura como particulas ordinarias del Modelo Estandar situadas en la brana. Se ha calculado el potencial y la fuerza efectiva sufridas por las particulas y las orbiras que estas siguen has sido dibujadas. Un experimento ideal se propone para el caso mas sencillo: situar solamente una particula en cada brana y dejarlas interactuar solamente mediante gravitacion. Diferencias entre este movimiento y el que generaria la ley de gravitacion de Newton son estudiados. Finalmente se comenta las posibilidades de detectar directamente o indirectamente estas particulas y, tambien, otros problemas aun sin resolver, en el marco de nuestro modelo.

# 1 Introduction and motivation

The Standard Model (SM) [1] is a relativistic quantum field theory with  $SU_C(3) \times SU_L(2) \times U_Y(1)$  gauge symmetry. It describes all of the fundamental interactions between elementary particles and all known particle physics phenomena with an incredible precision. The recent discovery of a particle with  $m_H = 125.3 \pm 0.4$  GeV, with the properties of the Higgs boson, confirms the electro-weak spontaneous symmetry breaking (SSB) of  $SU_L(2) \times U_Y(1) \rightarrow U_Q(1)$ , being  $U_Q(1)$  the electromagnetic charge group, and the Brout-Englert-Higgs mechanism [2, 3] to be responsible of W and Z masses.

However, there exist some experimental and theoretical evidences that force the SM to be extended in some way (see for example [4]).

## 1.1 Experimental problems of the Standard Model

We do know that the SM is not the ultimate theory mainly because of four experimental facts:

- Dark Matter: It is matter that we only have detected indirectly via its gravitational interaction. This matter does not emit electromagnetic radiation and because of that is called *dark*. Using Newton's law, we can compute the mass around which an object orbits by measuring its angular velocity with respect to the center of mass. We can also infer the mass of a star, or a galaxy, or a cluster of galaxies by measuring its luminosity. Comparing the mass of objects of different size computed in the two ways, it has been found that the angular velocity of objects far away from the center of mass around which they orbit was larger than expected. This can be understood assuming that there is more matter than what we expected, distributed in a big circular halo<sup>1</sup>. Dark matter is, therefore, another type of matter than we only detect gravitationally. The total density of baryonic matter is  $\Omega_B = 0.04$ , while there is a  $\Omega_{DM} = 0.23$  of dark matter. The evidence for DM in observations is overwhelming, starting with galaxy rotation curves, gravitational lensing and the Cosmic Microwave Background (CMB). While carefully concocted modified theories of gravity can perhaps explain almost all observations, the most accepted explanation lies in DM being composed mostly of cold, collisionless particles. The existence of dark matter implies the existence of physics beyond the SM. Firstly, it was thought that dark matter could be neutrinos, though now is known that dark matter moves slowly, at non relativistic velocities (at least, the major part of it), while neutrinos are ultra-relativistic because of its light mass. Hence, nowadays we think that dark matter is formed by much heavier particles. This hypothesis is known as Cold Dark Matter (CDM). CDM models propose that dark matter is non-dissipating and only can form big structures of galactic size.
- Baryogenesis: Processes that generated an asymmetry between baryons and antibaryons and that justify the excess of matter over antimatter in our present universe. Cosmic rays are a solid evidence that this asymmetry is maximal, i.e. practically there is no antimatter. There are two different ways of producing this asymmetry. The first one is that initially the baryonic symmetry was non-zero. The second one is that some phenomena that violates baryon number produced an imbalance that favoured the baryons. This could have happened in the first moments after Big Bang,  $t < 10^{-6}$  s. Both of these options are not experimentally excluded but the second one is preferred because theoretical prejudices suggest that an asymmetry previous to the Big Bang would be cancelled in the first moments after Big Bang. Andrei Sakharov postulated three necessary conditions for generating these imbalance, and these conditions imply necessarily new processes beyond the SM.
- Neutrino's masses: In the SM neutrinos were first considered as massless particles. However, it has been measured that neutrinos do have mass, more than 10000 times smaller than the electron mass

<sup>1</sup>We know that the dark matter creates an halo because gravitational lensing measurements.



[5]. We do not know yet the mechanism which give them mass, if they are Dirac or Majorana particles and if leptonic interactions involving neutrinos violate CP or not. We only know that new degrees of freedom must be added to the SM to give neutrinos a non-zero mass. Moreover, we can not explain the arbitrariness of the mass of SM fermions, spanning almost eleven orders of magnitude ( $m_\nu/m_e \sim 10^{-5}$   $m_\nu/m_\tau \sim 10^{-11}$ ). This last problem is also known as the *flavour problem*.

- Dark Energy: At present we know that the Universe is in accelerated expansion. Dark energy is the responsible of generating a negative pressure that generates this expansion. It is expected that the dark energy density is  $\Omega_{DM} \sim 0.73$ . Nowadays, we don not know much about dark energy. The density of dark energy ( $6.9110^{27} \text{ kg/m}^3$ ) is very low, smaller than the baryonic matter. However, it comes to dominate the mass-energy balance of the Universe because it is uniform across space.

## 1.2 The hierarchy problem

Due to all these experimental problems we think that the SM is an effective low energy theory of a more fundamental theory, and for this reason we look for SM extensions, i.e. models that includes the SM but explain also new things that the SM is not able to explain. However, when we assume that the SM is an effective theory, we face a new formal problem, known as the hierarchy problem.

Why gravity is so weak compared to the other three forces? The fact that an interaction is stronger than others is due to the couplings of the theory. We know that Newton's gravitation constant ( $G = 6.67 \times 10^{-11} \text{ Nm}^2 \text{ Kg}^{-2}$ ) is much smaller than, for example, Coulomb's constant ( $K = 9 \times 10^9 \text{ Nm}^2 \text{ C}^{-2}$ ). And why is this? In this section we will make a brief introduction to this problem, the hierarchy problem, problem with no solution yet and of great formal interest in physics.

We need to introduce in this section the concept of scale of a theory. When we refer to scale we refer to the energy below which a theory is applicable. We denote these theories as low-energy theories. If there exist a theory with a higher energy scale and that explain the same phenomena, we call this theory an ultraviolet extension or high-energy theory. For example, if we have a theory A with scale  $\Lambda$  and a theory B with scale  $\Lambda' > \Lambda$ , then theory B is an ultraviolet extension of theory A <sup>2</sup>. It is obvious that both theories predict the same at energies below  $\Lambda$ . Because of this, parameters of both theories must be related.

When fundamental scales of a Lagrangian differ in some orders of magnitude, we speak of a hierarchy problem. In particle physics the most important hierarchy problem is due to gravity and electroweak interactions. The symmetry breaking scale of electroweak interaction is  $\Lambda_{EW} \sim 250 \text{ GeV}$  while the scale of gravity is the Planck mass,  $M_P \sim 10^{19} \text{ GeV}$ . There exists a difference of 17 orders of magnitude between the scales of both theories. Moreover, it has been measured that the Higgs boson mass [6, 7] is  $m_H = 125.3 \pm 0.4 \text{ GeV}$ , i.e. is of the electroweak scale order. Radiative corrections to the Higgs boson mass, however, diverge quadratically,  $\delta m_H^2 = \mathcal{O}(\Lambda^2)$ . If the SM was a renormalizable theory this would not suppose a problem, because we can renormalize defining  $(m_H^{ph})^2 = m_H^2 + \delta m_H^2 = 125.3 \pm 0.4 \text{ GeV}$ . However, if we think that the SM is an effective theory of a more fundamental theory, radiative corrections acquire a natural cut-off [8] given by the first physics scale associated to this high-energy theory. If we suppose that there is nothing in these 17 orders of magnitude (physics desert) we would expect that the Higgs boson mass should be of order of the Planck mass,  $m_H^2 \sim \delta m_H^2 = c M_P^2$  (with  $c$  a real number to be determined) in contradiction with the experimental measure  $m_H^{ph}$ . In order that the Higgs boson mass be  $m_H^{ph} = \mathcal{O}(\Lambda_{EW})$ , being its radiative corrections  $\delta m_H^2 = \mathcal{O}(M_P^2)$ , there must exist a cancellation mechanism of this corrections at a  $1/M_P^2$  level, i.e.  $c \sim \Lambda_{EW}^2/M_P^2 \sim 10^{-34}$ . It is very unlikely that the coefficient  $c$  is so small with no reason, and for this is reasonable to assume that new physics exists between  $\Lambda_{EW}$  and  $M_P$ .

<sup>2</sup>Electroweak theory is an ultraviolet extension of electromagnetism and weak interaction, for example.

The hierarchy problem and the experimental evidences explained above make us think that the SM is not the ultimate theory, and make us look for SM extensions.

### 1.3 Possible solutions to the hierarchy problem

There are plenty of models that can solve the hierarchy problem, and have not been yet discarded by the LHC. The most important are built upon the following assumptions:

- Supersymmetry [9]: This class of models consider a new symmetry in which each particle has its own partner that satisfies a different statistics, i.e. each boson has a fermion partner and each fermion has a boson partner, with the same quantum numbers. This symmetry must be broken and, because of that, there is a difference in the masses of the supersymmetric partners. This is the reason why we have not found them yet. Supersymmetry allows to consider the ultraviolet cutoff  $\Lambda_{UV}$  of the SM to go until Planck's mass scale, because of the cancellation of the corrections to the Higgs mass produced by an opposite sign generated for the change on the statistics (fermions and boson give the same term but changing a sign) of supersymmetrical particles. In supersymmetric models new physics is expected in the region were LHC has been looking, and, therefore a serious tension between these models and data exist.
- Technicolor [10]: Considers that quarks are not fundamental particles and that they are formed by smaller particles, tied by a super-strong interaction. This theory tries to solve the symmetry breaking without introducing the Higgs mechanism. This theory considers a new gauge interaction, at 1 TeV and, therefore, avoids the hierarchy problem.
- Extra dimensions: This one is the possibility studied in this work and it is going to be exposed in more detail during the following sections.

### 1.4 LED model

The first theory including more than 4 dimensions was introduced in 1920 by the physicist Theodor Kaluza. He intended to unify gravity and electromagnetism introducing a new spatial dimension. He considered that every geodesic was in reality a cylinder, so the fifth dimension was a circle. Afterwards Oskar Klein introduced quantum mechanics in Kaluza's theory. This idea was abandoned because we do not know how to unify gravity with weak and strong interactions and we do not know how to quantize gravity.

The idea of extra dimensions was however retaken in the 80's by string theory. String theory need extra dimensions to achieve gravity quantization. Having string theory as a starting point, new models of field theories with extra spatial dimensions were proposed in the 90's. Some of them are Large Extra Dimensions [11, 12] that will be reviewed hereafter, Universal Extra Dimensions and Randall-Sundrum models[13, 14].

The Large Extra Dimension (LED) model was introduced by Ignatios Antoniadis, Nima Arkani-Hamed, Savas Dimopoulos and Gia Dvali in a series of papers and it is also known as ADD model.

Antoniadis, Dimopoulos and Dvali introduced in 1997 [11] scenario known as ADD, that was inspired in string theory. One year later these authors together with N. Arkani-Hamed [12] proposed the scenario that we will expose here (AADD). The main goal of this scenario is to solve the hierarchy problem without

new symmetries. This problem is solved through the existence of extra spatial dimensions. The spatial dimensions are compactified in a volume  $V_n$ , with  $V_n^{-1/n}$  being much smaller than the electro-weak scale,  $\Lambda_{EW}$  (i.e. the volume is large).

The main characteristic of this model is that only gravity can propagate along the extra dimensions. SM fields (that are represented by open strings in the fundamental theory) are attached to a D3-brane and can not escape from it<sup>3</sup>. Because of that we live in a 3+1 dimensional world and we observe that gravity is much weaker than the other forces, since the propagation along the extra dimensions produce a potential in  $4 + n$  dimensions and part of the gravitational field is dissipated through the extra dimensions. The relation between the gravitational scale that we observe ( $M_P$ ) and the real fundamental ( $M_D$ ) is:

$$\frac{1}{G_4} = \frac{1}{(G_D)^{\frac{n+2}{2}}} V^n \iff M_P^2 = M_D^{n+2} V^n, \quad (1)$$

where  $G_D$  is the gravitational constant in  $D = 4 + n$  dimensions and  $G_4$  is the normal Newton constant. For a big compactification volume the gravitational constant that we observe is much smaller than  $G_D$ . If we now consider<sup>4</sup>  $M_D \sim 1$  TeV, gravity will be unified with the gauge interactions. Compactifying to 3 spatial dimensions the unique way of obtaining a gravity scale much smaller than Planck's scale is having a huge compactification volume [15]. Then, the hierarchy problem is solved by annulment: when large extra dimensions exist, both interactions have a similar scale and there is not a big difference between  $\Lambda_{EW}$  and  $M_D$ .

## 1.5 Many-branes model

In the AADD model the  $n$ -dimensional bulk, that is the name that receives the  $4+n$  dimensional space, is considered to be empty, i.e. only gravity can feel its existence. However, nothing forbids the existence of other branes, distinct from our brane, at a distance  $d < 2\pi R$  (being  $R$  the compactification radius of the extra dimension). Actually, in string theory, many branes must be piled up to explain the observed gauge groups and it therefore seems a natural assumption to imagine several of these branes distributed along the extra dimensions. We consider, then, the existence of  $n$  extra spatial compactified dimensions, with common compactification radius  $R$ . We are not going to consider the possible existence of more temporal dimensions. SM fields, as always, are attached to a four dimensional object called brane (see section 2.1). Because of that we can only detect four dimensions. Gravity is the only interaction that can freely propagate into the bulk. Let's assume the existence of many branes and that in each brane there is certain amount of matter with the same gauge group as the SM. We can only interact with the matter in other branes via gravitation. Of course the bulk has no massive objects because gravity makes them fall into the branes after a certain amount of time, and it is safe then to consider an empty bulk.

The existence of SM-like matter in other branes that only interacts with us gravitationally can then explain the existence of DM: it would be normal baryonic matter that only interacts with us via gravitation, being attached to a different brane. The goal of this work is to introduce the idea and start to expose its consequences. For simplicity we will work with only one extra dimension. Therefore, being current data on deviation from Newton's law excluding compactification radii  $R > 40\mu\text{m}$ , it is impossible to solve the hierarchy problem, as  $M_D$  will be typically  $M_D \sim 10^8$  GeV. However, if more than one extra dimension is considered, then this hypothesis could both offer a DM candidate and solve the hierarchy problem.

In section 2 we will introduce the necessary ingredients for our work, we will derive the potential and compute the force for bodies in a 5 compactified dimensional space. We will also expose the experimental

<sup>3</sup>Concepts like open string or brane are explained in section 2.1.

<sup>4</sup>A value of  $M_D \sim 1$  TeV is selected because is the typical energy that we can test at the LHC.

bounds on the existence of extra compactified dimensions.

On the other hand, in section 3 we will present our results on an interesting *gedanken experiment*. We will study what happens if we locate just one particle in our brane and just one particle in another brane at a distance  $d < 2\pi R$ . We will study the differences between the movement caused by a mass located in the other brane and the newtonian movement with two masses located at the same brane.

In section 4 we will briefly sketch the work that must be done to compare our hypothesis with data concerning angular velocities of stars and galaxies, the cosmic microwave background, the baryon acoustic oscillations and direct and indirect observation of DM particles. All these searches require an amount of work that exceeds the possibility of this short work, and it will be pursued in the future.

## 2 Gravity in presence of two or more branes

In this section we introduce our hypothesis, i.e. that several branes (a concept reviewed in Section 2.1) are present in a  $n$ -dimensional bulk compactified in a  $n$ -tori with common radii  $R$ . On the different branes, SM-like matter and gauge fields can be distributed much as in the case of our brane, thus forming structures at different scale as in our Universe, from stars to cluster of galaxies. This matter is only felt gravitationally by matter located in our brane and, thus, can be understood as *Dark Matter*. This hypothesis was advanced in Ref. [16] and suggested in scientific and non-scientific papers at the end of the 90's but, to our knowledge, has not been investigated further in the last 15 years.

The section is organized as follows: in Section 2.1 we introduce the concept of brane; in Section 2.2 we remember how the compactification radius and the fundamental gravitational scale  $M_D$  depends on the number of extra dimensions; in Section 2.3 we compute the gravitational potential in presence of one extra compact dimension; in Section 2.4 we compute the gravitational force in presence of one extra compact dimension for bodies located on the same brane, in the brane and in the bulk or on two different branes; in Section 2.5 we explain how the present bounds on  $R$  can be obtained by studying the potential computed in Section 2.3.

### 2.1 Concept of brane

In string theory initially were proposed open and closed strings. Both are fundamental point like objects [17, 18]. An open string has two ends, it is topologically the same as a line. In contrast a closed string has no ends and is topologically the same as a circle. However this objects were not enough to describe completely the theory.

Soon was known that energy was able to propagate along an open string. So a problem emerge when this energy arrived at one end of the string. When the energy arrived to the end of the string this energy disappeared. Energy conservation can not be violated. In order to avoid this problem the theory must introduce some other object. This objects are  $D$ -branes and  $p$ -branes.

The  $p$ -branes are objects with  $p$  dimensions that live in a space with  $n \geq p$  spatial dimensions. For example a 0-brane is a point, while a 2-brane is a membrane.  $D$ -branes [19, 20] are a peculiar type of  $p$ -branes.  $D$ -branes are topologically extended defects, with the property that strings can link up them, satisfying Dirichlet boundary conditions in their ends. So when one or some string link up a  $p$ -brane they form a  $D$ -brane. For consistence of the theory we need all open string to be linked up to some  $D$ -brane. The dimension of the  $D$ -brane is indicated putting the number of spatial dimensions after the  $D$ .

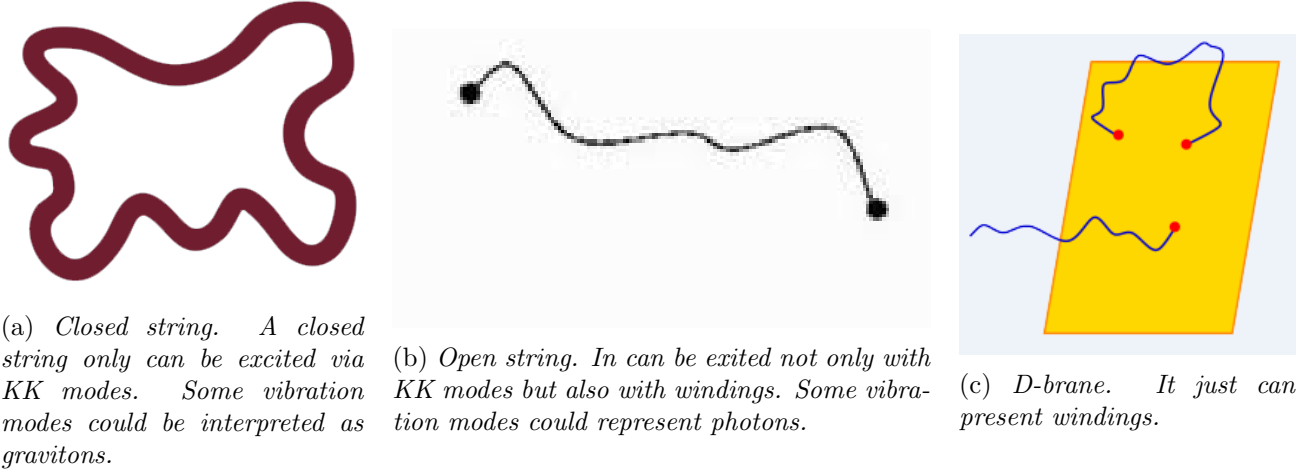


Figure 1: *Objects present in string theory and how can they be excited.*

In figure 1 the different objects and also they different fluctuations of the theory are shown. These objects are closed strings (a), open strings (b) and D-branes (c). Commonly we will call D-branes just as branes. There are two types of fluctuations that these objects may have:

- KK modes. They are the excitations than an object receive when he moves around the compactified dimension. This modes were first derived by Kaluza and Klein, and their mass is inversely proportional to the compactification radius. Both closed and open strings can present KK modes. Gravitons are often represented by closed strings, so gravitons could have KK modes.
- Windings. Punctual particles can only present KK modes in compactified dimensions. They only can move in the space. However extended objects, like strings, can wind along the compactified dimensions (see Figure 2). This possibility generates a new way of exciting these objects, the winding modes. Their mass is proportional to the compactification radius. This excitations can be suffered by D-branes and by open strings<sup>5</sup>.

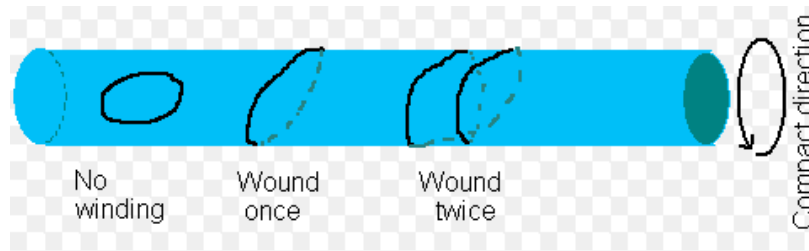


Figure 2: *Winding mode.*

## 2.2 R dependence on n

We introduce now how the compactification radius depends on the numer of extra compactified dimensions and on the value elected of  $M_D$ . As we have said, in this work we are not particularly interested in decreasing the scale of the theory  $M_D$  until 1 TeV, but in introducing a solution to DM. Because of that we are going to study the easier case, with only one extra dimension  $n = 1$ , and choose a scale such

<sup>5</sup>Closed strings can wind but they do not present winding modes because their centre of mass can not change.

$x$	0	1	2	3	4	5	6
$M_D(\text{TeV})$	1	10	100	1000	$10^4$	$10^5$	$10^6$
$R \text{ (cm)}$	$10^{13}$	$10^{10}$	$10^7$	$10^4$	10	$10^{-2}$	$10^{-5}$

Table 1: Compactification radius for one extra dimension depending on the value chosen for  $M_D$ . First considered in LED by AADD.

that the compactification radius is smaller than the shortest distance where gravity has been measured experimentally. This distance is  $R_{exp} \sim 50\mu\text{m}$ .

Starting from the equation that relates the Planck's mass in four dimensions and in  $4 + n$  dimensions we want to calculate the bounds on the compactification radius. This equation is:

$$M_P^2 = M_D^{2+n} V^n . \quad (2)$$

So, if we choose a  $M_D = 10^x \text{ TeV}$  the compactification radius will be given by the formula:

$$R_n = 10^{\left(\frac{30-x(2+n)}{n}-17\right)} \text{ cm} . \quad (3)$$

The different compactification radius for the case of  $n = 1$  are exposed in Table 1. We appreciate that to avoid the experimental bound we need for one extra dimension the gravity scale to be at least  $M_5 > 10^5 \text{ TeV}$ . In Section 3, where we develop our model, we will choose a value of  $M_5 = 2 \times 10^5 \text{ TeV}$ , that corresponds to a compactification radius of  $R = 10\mu\text{m}$ , that is one order of magnitude lower than the experimental bound. Take into account that we are not solving the hierarchy problem, but we are still lowering gravity scale is almost 11 orders of magnitude.

### 2.3 Gravitational potential in five dimensions

When the original Large Extra Dimensions model was presented in Refs. [21, 12], a simple phenomenological potential was derived in the limit of very large standard dimensions  $r = |\vec{r}|$  with respect to the average compactification radius  $R = |\vec{R}|$ ,

$$V_{4+n}(|\vec{r}| \gg |\vec{R}|) \sim -\frac{m}{M_D^{2+n} R^n r} \sim -\frac{m}{M_P^2 r} , \quad (4)$$

where the mass  $m$  is the source of the gravitational field and  $M_P$  and  $M_D$  are the Planck mass and the fundamental scale of gravity in  $D = 4 + n$  dimensions, respectively. The last equation establishes a relation between the two scales:

$$M_P^2 \sim M_D^{2+n} R^n , \quad (5)$$

so that the Planck scale can be much higher than the fundamental scale of gravity  $M_D$  if the compact volume  $V_n \propto R^n$  is large, thus solving the hierarchy problem. In a subsequent paper, Ref. [22], the size of the first order corrections in  $|\vec{r}|/R$  was also sketched:

$$V_{4+n}(|\vec{r}| \gg |\vec{R}|) \simeq -\frac{m}{M_P^2} \sum_{(k_1, \dots, k_n)} \frac{e^{-2\pi L |\vec{k}|/r}}{r} . \quad (6)$$

A complete computation of the gravitational potential in the case of  $\mathcal{M}_4 \times \mathcal{S}_n$ <sup>6</sup>, however, was only given in Refs. [23, 15]. A very simple derivation of the potential can be found in Ref. [16] and it is outlined below for the case at hand of one compact extra-dimension, only.

Consider, first, the gravitational potential in 5 non-compact dimensions:

$$V_5^{\text{non-compact}}(a, y) = -\frac{G_5 m}{2} \frac{1}{[a^2 + y^2]}, \quad (7)$$

where  $l = \sqrt{a^2 + y^2}$  is the distance from the source of the potential, divided into its three-dimensional projection  $a = |\vec{a}|$  and its extra-dimensional component,  $y$ . The 5-dimensional Newton constant,  $G_5$ , has the dimensions of  $M_D^{-3}$ , being  $M_D$  the fundamental scale of gravity.

Notice, however, that if we consider now an extra-dimension compactified on a circle of radius  $R$ , the path of length  $l$  is not the only one that connects the mass  $m$  with the source of the potential: we can reach the source of the potential by travelling along a straight line *wrapping* around the compact dimension as many times as we want (see Appendix B). The length of a path that goes  $m$  times around the compact dimension is  $l_m = \sqrt{a^2 + (y - 2\pi R m)^2}$ . Therefore, the source is effectively *felt* by the mass  $m$  infinitely many times, albeit the gravitational potential is increasingly feeble as long as we turn more and more. In order to compute the full gravitational potential felt by  $m$  in a compact space-time, we can imagine an infinite extra-dimension  $y$  with an infinite number of sources located at distance  $2\pi R$  from each other, and just sum their potentials:

$$V_5^{\text{compact}}(a, y) = -\frac{G_5 m}{2} \sum_{k=-\infty}^{\infty} \frac{1}{[a^2 + (y - 2\pi R k)^2]}, \quad (8)$$

where the sum goes from  $-\infty$  to  $+\infty$  since we can wrap around the compact dimension travelling in both directions. Define  $L = 2\pi R$  the length of the compact dimension. Then, use the following identity:

$$\frac{1}{a^2 + (y - Lk)^2} = \frac{1}{2iLa} \left( \frac{1}{k + z} - \frac{1}{k + z^*} \right), \quad (9)$$

where

$$z = -\frac{y + ia}{L}. \quad (10)$$

The potential can thus be written as:

$$V_5^{\text{compact}}(a, y) = -\frac{G_5 m}{4iLa} \sum_{k=-\infty}^{\infty} \left( \frac{1}{k + z} - \frac{1}{k + z^*} \right), \quad (11)$$

an expression that can be easily summed since:

$$\sum_{k=-\infty}^{\infty} \frac{1}{k + z} = \pi \cot \pi z, \quad (12)$$

---

<sup>6</sup>This is the metric,  $\mathcal{M}_4$  corresponds to Minkowski metric in four flat dimensions, and  $\mathcal{S}_n$  to  $n$  dimensions compactified in circles.

and, therefore,

$$V_5^{\text{compact}}(a, y) = -\frac{G_5 m}{8iRa} (\cot \pi z - \cot \pi z^*) . \quad (13)$$

After some algebraic manipulation, we get:

$$V_5^{\text{compact}}(a, y) = -\frac{G_5 m}{4Ra} \left[ \frac{\sinh\left(\frac{a}{R}\right)}{\cosh\left(\frac{a}{R}\right) - \cos\left(\frac{y}{R}\right)} \right] . \quad (14)$$

This potential calculated by [16] is identical to the one calculated by [15] which is:

$$V_5 = \frac{1}{M_{P_5}^3} \frac{1}{2aR} \left( 1 + 2 \frac{e^{\frac{a}{R}} \cos \frac{y}{R} - 1}{e^{2\frac{a}{R}} - 2e^{\frac{a}{R}} \cos \frac{y}{R} + 1} \right) . \quad (15)$$

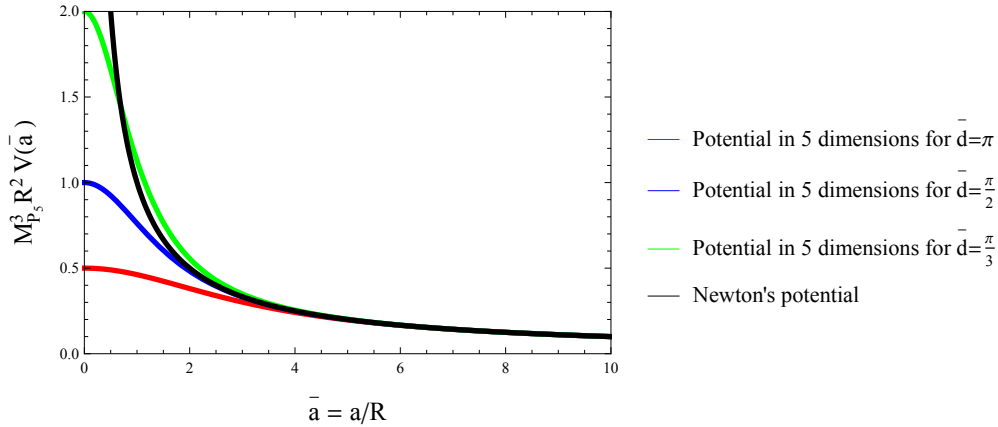


Figure 3: *Potential with one extra compactified dimension and newtonian potential. Notice that for small values of  $\bar{d}$  ( $\bar{d} < \frac{\pi}{2}$ ) the potential becomes stronger than Newton's potential for distances  $1 < \bar{a} < 4$ .*

This potential is shown for different values of  $\bar{d} = \frac{d}{R}$  in figure 3. Observe that for smaller values of  $\bar{d}$  the potential becomes stronger at small distances. For distances  $\bar{a} > 5$  the potential is equal to Newton's potential and the value of  $\bar{d}$  is irrelevant. The potential for  $\bar{d} = 0$  is plotted in figure 4. This potential is the one in which we are interested experimentally.

In Figure 5 the potential in five dimensions with the extra dimension compactified with a radius  $R$  is plotted in two interesting limits: big distances limit and short distances limit, both in comparison to the radius  $R$  (these limits are computed hereafter). In this figure is shown that the potential at big distances follows the classic Newtonian potential, i.e. at big distances the extra dimension is not seen. On the contrary at short distances the potential tends to  $\frac{cmt}{r^2}$  law, i.e. at short distances the potential does not see the compactification of the extra dimension. We say this because Gauss law in  $3+n$  spatial dimensions will give as a potential of the form:

$$V_{3+n} = \frac{MG_{4+n}}{r^{n+1}} \quad (16)$$

This explains why if  $R$  is small (of the order of  $10 \mu m$ ) we do not perceive the extra compactified dimensions, because we live in the big distances limit. It would be interesting to study in more detail the short distances limit. It would be also interesting to propose experiments that improve this results. This



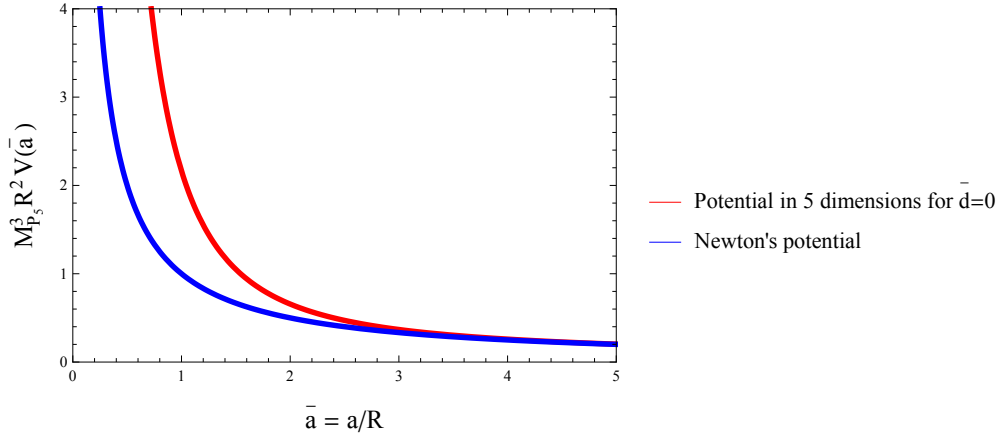
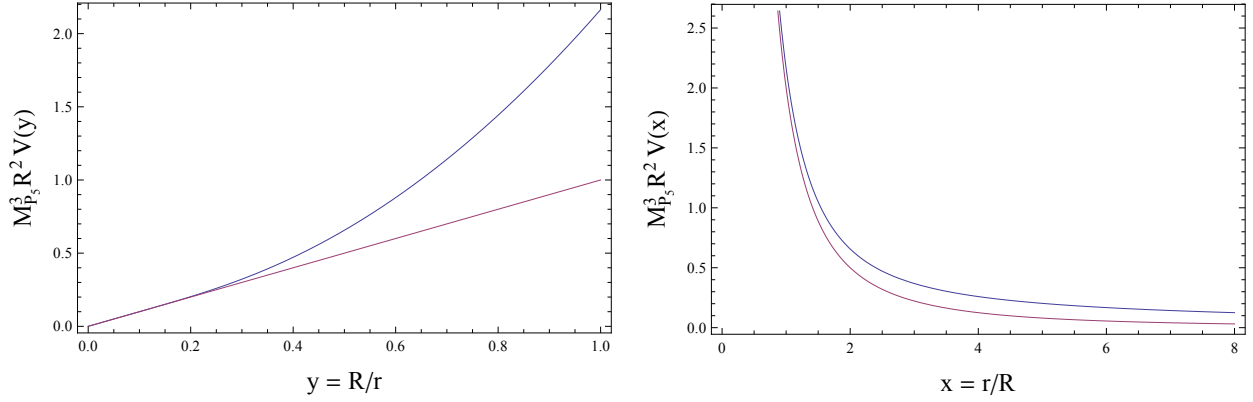


Figure 4: Comparison of the potential with one extra compactified dimension and newtonian potential. Is the relevant case for experiments, i.e. the case in which both particles are in the same brane,  $d = 0$ .



(a) Potential in 5 dimensions (blue line) and  $\frac{1}{r}$  (purple line). This figure corresponds to the big distances limit.

(b) Potential in 5 dimensions (blue line) and  $\frac{1}{r^2}$  (purple line). This figure corresponds to the small distances limit.

Figure 5: Modulus of the 5 dimensional potential, both considering that there is no distance between the two branes  $d = 0$ . In figure (a) it is shown how the potential tends to classic Newtonian potential at big distances compared with the compactification radius, while in figure (b) shows the small distances limit and how the potential tends to  $\frac{1}{r^2}$ .

corrections at small and big distances compared with the compactification radius are going to be discussed now in more detail.

### 2.3.1 Corrections at big distances

Here we are going to consider the development of the potential at distances much bigger than the compactification radius ( $a \gg R$ ). Because we are considering small compactification radius of micrometer distances, this approach is the one we should measure, and it is given by the expression:

$$V_{4+n}(|\vec{a}| \gg |\vec{R}|) \sim -\frac{m}{M_D^{2+n} R^n a} \sim -\frac{m}{M_P^2 a}, \quad (17)$$

that is the newtonian potential in 4 dimensions. A more general formula is given if we take into account the next order:

$$V_5^{\text{compact}}(a \gg 1, d) \sim -\frac{G_5 m}{4R^2 a} [1 + 2 \cos d \times e^{-a} + \dots] . \quad (18)$$

This potential will be the one we will use to look for deviations to Newton's law. It is developed in more detail in section 2.5.

### 2.3.2 Corrections at small distances

For two masses located on the same brane,  $y = 0$ , at very short three-dimensional spatial distance from the source we get:

$$V_5^{\text{compact}}(a \ll 1, 0) \sim -\frac{G_5 m}{2R^2 a^2} + \mathcal{O}(a) , \quad (19)$$

i.e. the non-compact 5-dimensional potential of equation 7. On the other hand, when  $y \neq 0$ , the potential is quite different:

$$V_5^{\text{compact}}(a \ll 1, d) \sim -\frac{G_5 m}{4R^2(1 - \cos d)} + \mathcal{O}(a) , \quad (20)$$

and it is dominated by a volume term depending on the size of the extra-dimension. Notice that, since the gravitational force attracts necessarily a body in the bulk towards the source of the potential, considered fixed onto a brane,  $y \rightarrow 0$  and, therefore, at some point eq. (7) is recovered.

## 2.4 Force

In this section we are going to calculate the force on a particle (particle 1) of mass  $m$  placed in the brane in  $y = 0$  caused by a particle (particle 2) of mass  $M$  placed in  $y = d$  in the extra dimension. We also will study the difference in the force depending on if particle 2 is in the brane or it is in the bulk.

The potential is:

$$V_5 = -\frac{G_5 M}{2} \sum_{m=-\infty}^{\infty} \frac{1}{[a^2 + (y - 2\pi R m)^2]} = -\frac{G_5 M}{2} \sum_{m=-\infty}^{\infty} \frac{1}{r_m^2} \quad (21)$$

where the distance  $r$  depends on the winding  $m$ . The force would be the potential gradient. The force is, then:

$$\vec{F}_5 = -\vec{\nabla} V_5 = -G_5 M m \sum_{m=-\infty}^{\infty} \frac{1}{[a^2 + (y - 2\pi R m)^2]^{3/2}} \hat{r} = -G_5 M \sum_{m=-\infty}^{\infty} \frac{1}{r_m^3} \hat{r} , \quad (22)$$

that can be computed deriving the potential arriving to the expression:

$$F_5(r) = \frac{G_5 M m}{4R^3} \frac{1}{\bar{a}^2} \left[ \frac{\cosh \bar{a}}{\cosh \bar{a} - \cos \bar{d}} - \bar{a} \frac{1 - \cosh \bar{a} \cos \bar{d} - \sinh \bar{a} \cos \bar{d}}{(\cosh \bar{a} - \cos \bar{d})^2} \right] . \quad (23)$$

where  $\bar{a} = \frac{a}{R}$ . However, if the particle is not in the bulk and it is located onto a brane, the brane causes that the effective force goes in the brane direction  $\hat{a}$ , similar to what happens in an inclined plane. The effective brane-to-brane force,  $F_{BB}$  is therefore:

$$\vec{F}_{BB} = -\vec{\nabla}_a V_5 = \left( \frac{\partial}{\partial \hat{a}} V_5 \right) \hat{a} = -G_5 M m \sum_{m=-\infty}^{\infty} \frac{a}{[a^2 + (y - 2\pi R m)^2]^2} \hat{a} = -G_5 M \sum_{m=-\infty}^{\infty} \frac{a}{r^4} \hat{a}, \quad (24)$$

that also can be calculated as:

$$\vec{F}_{BB} = -|\vec{F}_5| \cos(\theta_m) \hat{a} = -|\vec{F}_5| \frac{a^2}{r^2} \hat{a}. \quad (25)$$

Observe that in the limit of  $y \ll a$  we have  $a \simeq r$  and the effective force is that in 5 dimensions without brane. The force can be calculated deriving the potential but without the derivative in the extra dimension. We obtain:

$$F_{BB}(\bar{a}, \bar{d}) = -\frac{G_5 M m}{4R^3} \frac{1}{\bar{a}^2} \left[ \frac{\cosh \bar{a}}{\cosh \bar{a} - \cos \bar{d}} - \bar{a} \frac{1 - \cosh \bar{a} \cos \bar{d}}{(\cosh \bar{a} - \cos \bar{d})^2} \right] \hat{a}. \quad (26)$$

This force is not singular unless we consider  $d = 0$ , i.e. just one brane. We appreciate that the force tends to zero at big distances but also is zero when  $a = 0$ . For the validity of the model the force must tends to Newton's law at ordinary distances.

The differences between the two forces are evident: in equation 22 we appreciate that the force goes in the direction that joins both particles, as it happens commonly in central forces. However, in equation 24 we observe that the force is not central, i.e. goes along the brane direction and not in the radial direction. This is similar at what happens with an inclined plane: when we constrain the particle to a surface it can not cross through, and then rolls along the constrain. Observe that if one particle is initially into the bulk it will collapse into a brane because of the gravitational attraction of the particles located into the branes.

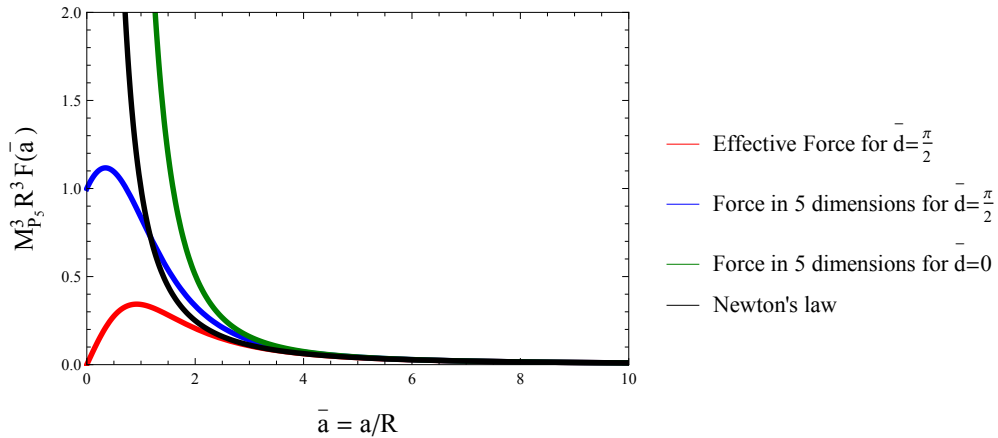


Figure 6: Comparison of the different forces. Effective force  $F_{BB}$  is shown to be different from 5 dimensional force. Both tend to the newtonian force in four dimensions for distances  $a > 4R$ . The effective force for  $d = 0$  is the same as the force in 5 dimensions for  $d = 0$ , and it is divergent (diverges quadratically).

Experimentally we could put to masses at small distances and study the force exercised between them. This case is the one  $d = 0$  and is also plotted in figure 6. The difference between them is relevant only at distances of order of the compactification radius.

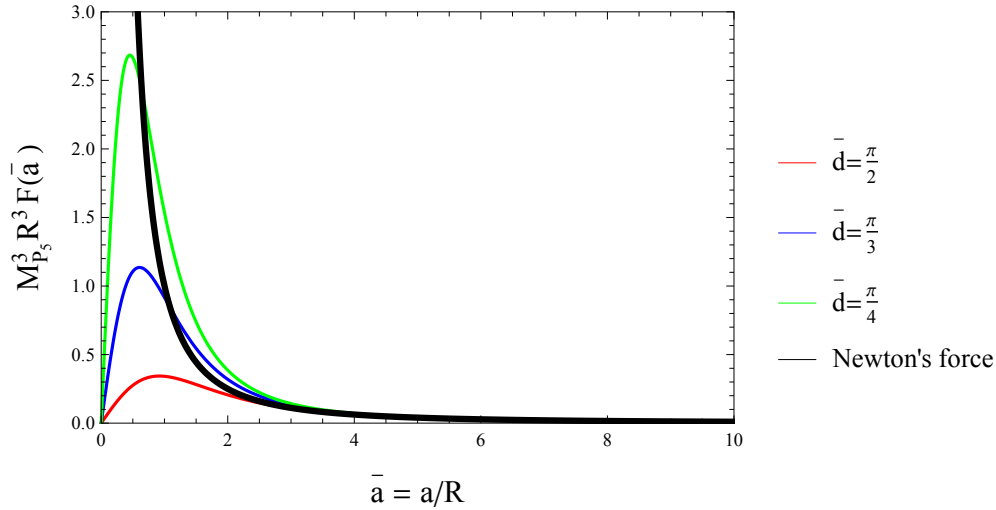


Figure 7: We show here the dependence of the force along the brane with the distance between the two branes. We can see that for smaller values of  $\bar{d}$  the force becomes stronger at small distances.

#### 2.4.1 Corrections at big distances

Here we are going to consider the development of the force at distances much bigger than the compactification radius ( $r \gg R$ ). Because we are considering small compactification radius of micrometer distances, this approach is the one we should measure. We start considering the expansion for  $\bar{a} \gg 1$  and  $\bar{d} \ll 1$ , we find:

$$F_{BB} = \frac{G_5 M m}{a^2} , \quad (27)$$

that is the Newton force in 4 dimensions. It is what we expected, we find the same result that we obtained for the potential. At big distances we have to reproduce Newtons law, that is what we observe at distances grater than a few micrometers.

#### 2.4.2 Corrections at small distances

Here we are interested in two particular cases: how the force evolves when only  $\bar{a}$  is small and how it varies for small radial distances. For  $\bar{a} \ll 1$  and  $\bar{d} \simeq \pi$ , we find:

$$F_{BB} = G_5 M m \frac{a}{12} (1 + (d - \pi)^2) . \quad (28)$$

However if we study the case of the expansion for  $\bar{a} \ll 1$  and  $\bar{d} \ll 1$ , we find:

$$F_{BB} = G_5 M m \left( \frac{4a}{d^4} + \frac{a}{180} + \frac{ad^2}{756} \right) . \quad (29)$$

What we are finding here is also the same that we found for the potential. For small distances we can see the compactification of the extra dimension. We also have seen that at small distances the brane position becomes relevant. If we study the force at big distances the position of the brane can be disregarded.

$n$	1	2	3	4	5	6	$\infty$
$R$ (cm)	$10^{13}$	0.01	$10^{-7}$	$3 \times 10^{-10}$	$10^{-12}$	$10^{-13}$	$10^{-17}$

Table 2: Compactification radii depending on the number of extra dimensions considered. First considered in LED by AADD.

## 2.5 Bounds on $R$

To solve the hierarchy problem we must find a measurable value for  $M_D$ . With the new run of the LHC we are going to arrive to energies os almost 14 TeV. If we postulate that  $M_D = 1$  TeV using equation 2 we find for  $R$ :

$$R_n = 10^{(-17 + \frac{30}{n})} \text{ cm} . \quad (30)$$

With this formula we can calculate the compactification radius in function of the number of the extra compactified dimensions. For simplicity we are taking into account that all the dimensions have the same compactification radius. In Table 2 we show the different radius until  $n = 6$  extra dimensions.

We notice that the case with just one extra dimension must be excluded. This radius should have produced deviations to Newton's law at solar system distances. For saving experimentally this case we must increase  $M_D \sim 10^5$  TeV. If we consider  $n = 2$  we obtain a radius of 0.1 mm. The shortest distance where gravity has been measured is more or less  $50 \mu\text{m}$ , so this case is also excluded if we consider  $M_D = 1$  TeV. However if we allow  $M_D$  to increase until a few TeVs a scenario with two extra dimensions would be also possible. We also appreciate that for infinite extra dimensions the compactification radius tends to the Planck's mass.

Deviations from Newton's law are commonly parametrized via a Yukawa type potential. Yukawa potential has two parameters,  $\alpha$  that represents the strength of the potential and  $\lambda$  that is the range of the potential:

$$V(r) = -\frac{G_4 M}{r} (1 + \alpha e^{-\frac{r}{\lambda}}) . \quad (31)$$

Experimentally we can study what potential generates one particle over another. The only set up that we can control is locating both masses in our brane, i.e. the case with  $d = 0$  (this result is the same that in equation 37 but without the cosine). In LED scenario corrections to Newton's law for  $d = 0$ , as we have seen, are given by the following potential:

$$V_{r>R} \sim \frac{1}{R^n r} \left( 1 + 2ne^{-\frac{r}{R}} \right) , \quad (32)$$

because of that  $\lambda \equiv R$  and  $\alpha = 2n$ . In figure 8 the experimental bounds for  $\alpha$  and  $\lambda$  are shown. The region of interest of the extra dimensions model is  $1 < \alpha < 10$ .

Experimentally the major problem to test gravity at small distances for atom to atom interaction, is that for small distances Van der Waals forces become of the same order of gravitational forces. At  $100 \mu\text{m}$  both interactions are more or less equal. However, Van der Waals forces decay with the seventh power when we increase the distance, so they are negligible for millimeter distances but really important for micrometer distances. In our model, on the other hand, no forces but gravitational interactions are felt

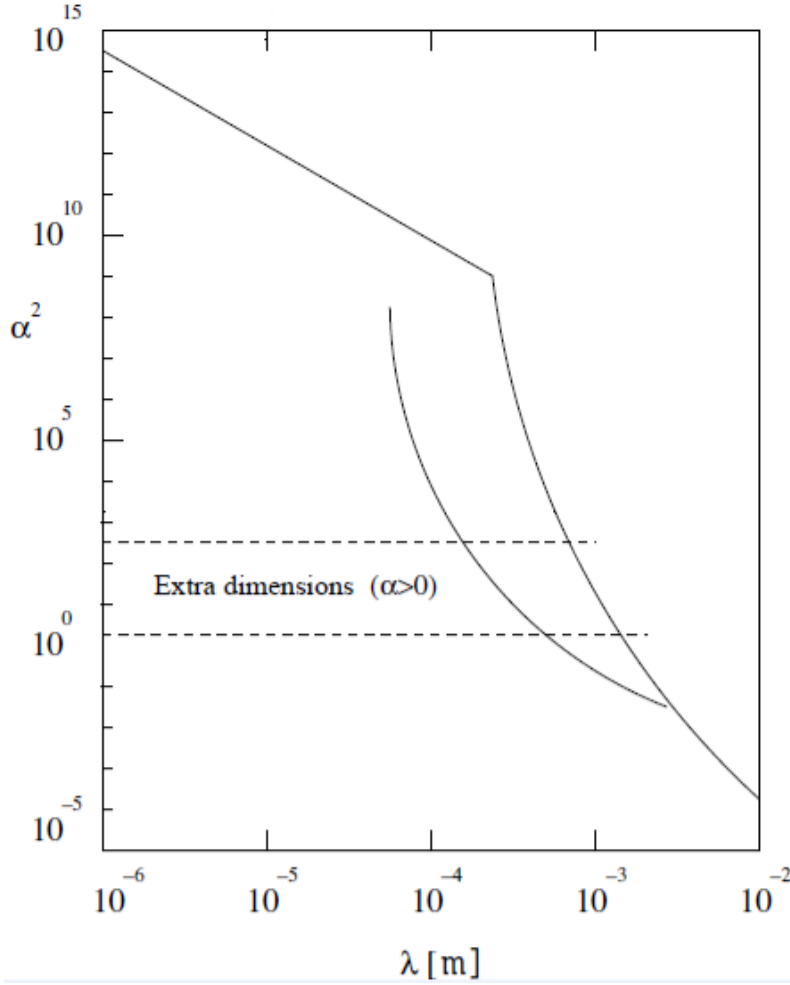


Figure 8:  $\alpha - \lambda$  diagram [23]. The lines show the experimental bounds for the compactification radius. They have been computed measuring gravity at short distances.

by particles located on two different branes. The two particles, in principle, could be as near as being one on top of the other (with a null force acting on them, as the gravitational force is exactly cancelled by the constrain represented by the branes).

### 3 Deviations from newtonian gravity: a *gedanken experiment*

In this section we develop our model and show the results that we have obtained. We consider here a scenario with only one extra dimension. Solving the hierarchy problem is not possible with just one extra dimension (see section 2.5). We are going to choose a  $G_5$  such that the compactification radius for one extra dimension is fixed to be  $R = 10 \mu\text{m}$ . This case implies that the scale of the theory is  $M_D \sim 10^5$  TeV. This scale can not be reached by the LHC but guarantees us that  $R$  is below the minimal distance at which gravity has been tested.

Our *gedanken experiment* is the following: imagine we have two particles of mass  $m$  (particle 1) and  $M$  (particle 2) located on two different branes at distance  $d$  in one extra compactified dimension of length  $L = 2\pi R$ , with  $R = 10\mu\text{m}$ . Within this hypothesis,  $M_D = 2 \times 10^5$  TeV, i.e. it is too large to solve completely the hierarchy problem (but we are lowering the scale almost 14 orders of magnitude still). Now, we can ask ourselves if the motion of the particle 2 on brane 2 in the frame in which particle 1 on brane 1

is at rest differs from what should occur if particle 2 and particle 1 were in the same brane. Is it possible to numerically differentiate the two scenarios? We will also compute the differences between this movements and those generated by Newton's law.

In this section we are going to proceed in the following way: firstly, in section 3.1 we will see the radial case and introduce the scenario; afterwards, in section 3.2, we will introduce an angular momentum term and we will solve numerically the differential equation; and, eventually, in section 3.3 we will see the differences in the orbit for both movements, that caused by Newton's law, and that caused for a five dimensional potential with two branes.

### 3.1 Falling towards a dark matter particle

First, we are going to solve the easiest scenario: one particle of mass  $m$  without initial transverse velocity interacting with a much heavier particle of mass  $M$ . We work in the reference frame in which the mass  $M$  does not move. In the classical scenario both bodies will collide, but if the bodies are placed in different branes an oscillatory movement will result. Consider first the case in which space-time is 3+1 dimensional. Newton's second law gives us the relation:

$$\vec{F}_4 = m \ddot{\vec{x}} , \quad (33)$$

where  $\vec{F}$  is the gravitational force in the direction going from  $M$  to  $m$ , and  $\vec{x}$  the position of the particle. We will restrict to a one-dimensional movement:

$$-\frac{G_4 M m}{a^2} = m \ddot{a} , \quad (34)$$

where  $a$  is the distance between the two particles. The expression can also be written as:

$$\ddot{a} + \frac{G_4 M}{a^2} = 0 . \quad (35)$$

In case in which  $m$  is located on a brane is an extra (compactified) equation 33 becomes:

$$\ddot{a} + \frac{G_5 M}{4Ra^2} \left[ \frac{\cosh \frac{a}{R}}{\cosh \frac{a}{R} - \cos \frac{d}{R}} - \frac{a}{R} \frac{1 - \cosh \frac{a}{R} \cos \frac{d}{R}}{(\cosh \frac{a}{R} - \cos \frac{d}{R})^2} \right] = 0 , \quad (36)$$

where, we remind,  $a$  is the 5-dimensional distance between  $M$  and  $m$  along the direction corresponding to the projection of  $(\vec{x}, y)$  along the standard 3-spatial dimension. As we saw in section 2.4.1 for larger distances compared to the compactification radius, the potential that a particle in a 5-dimensional space feels is:

$$V_5^{\text{compact}}(a \gg 1, d) \sim -\frac{G_5 m}{4R^2 a} . \quad (37)$$

As we have said, at big distances we have to reproduce newtonian gravity. This enables us to write the relation:

$$\frac{G_5 M}{4R^2 a} = \frac{G_4 M}{a} \longleftrightarrow \frac{G_5}{4R^2} = G_4 , \quad (38)$$

that is nothing but equation 2. We can see that the constant that multiplies both potential (and hence both forces) is the same if we consider the same mass generating the gravitational interaction. As we are interested in testing gravity at distances of a few microns, we are going to select a mass such that produces orbits of this size. For simplicity, then, we decided to select a mass<sup>7</sup> such that  $M = 10^{-7}$  Kg. This mass is really small for daily aspects, but it is really big for atomic distances, and fits perfectly to the type of experiment that we are interested in.

### 3.2 Orbiting around a dark matter particle

After the introduction done in the previous section now add an angular velocity. The motion becomes, then, now is in two-dimensions. We choose for simplicity polar coordinates:  $a$  is the radius of the orbit and  $\theta$  the angular coordinate. If we add an orbital velocity the differential equation changes. The coupled differential equations to solve are now:

$$\begin{cases} m\ddot{a} = \frac{l^2}{m^2} \frac{1}{a^2} \frac{d^2}{d\theta^2} \frac{1}{r} \\ a\dot{\theta} = \frac{l^2}{m} \frac{1}{a^3} \end{cases} \quad (40)$$

The radial equation can be written as in the previous section, but with a new term due to the angular momentum.

$$m\ddot{a} = F(a) + \frac{l^2}{ma^3} , \quad (41)$$

with  $l = m\dot{\theta}a^2$  being a constant fixed by the initial conditions of the system. Conservation of  $l$  is nothing else than angular momentum conservation. We recover equation 35 if  $l = 0$ . The presence of the brane does not spoil angular momentum conservation. If needed, once we have solved the radial equation we would be able to obtain  $\theta(t)$  using that:

$$\theta(t) = \int dt \frac{l}{ma^2(t)} . \quad (42)$$

For a newtonian movement the equation is:

$$\ddot{a} + \frac{G_4 M}{a^2} - \frac{l^2}{ma^3} = 0 , \quad (43)$$

whereas for the movement in the brane:

$$\ddot{a} + \frac{G_5 M}{4Ra^2} \left[ \frac{\cosh \bar{a}}{\cosh \bar{a} - \cos \bar{d}} - \bar{a} \frac{1 - \cosh \bar{a} \cos \bar{d}}{(\cosh \bar{a} - \cos \bar{d})^2} \right] - \frac{l^2}{ma^3} = 0 , \quad (44)$$

For a newtonian movement the orbit is given by the expression:

$$a(\theta) = \frac{\alpha}{1 + \epsilon \cos \theta} , \quad (45)$$

---

<sup>7</sup>This mass has been elected because allows us to write

$$\ddot{a} + \frac{1}{a^2} = 0 \quad (39)$$

if we put the distance in  $\mu\text{m}$ .



with  $\alpha = \frac{l^2}{mk}$ ,  $k = G_4 M$  and  $\epsilon = \sqrt{1 + \frac{2El^2}{mk^2}}$  being  $E$  the total energy of the particle. When the mass  $m$  is located on a second brane, its motion around  $M$  is still confined to its own 3-dimensional volume. However, the solution can not be easily computed and equation 36 must be solved numerically. In both cases the motion can be hyperbolic, parabolic or elliptic, depending on the initial conditions. We are going always for simplicity to choose  $\dot{a}(0) = 0$ , so at  $t = 0$  we only have transverse velocity.

Notice that if the particles are placed in different branes no residual interactions appear in the experiment. In common gravitational experiments it is really difficult to remove electromagnetic, weak and strong interactions and Van der Waals forces, that limit the minimum distance of which we can draw two particles near. However, in our experiment all these problems disappear due to the presence of the branes, that prevents the propagation of the gauge interactions. Notice also that we can not manipulate the masses in the other brane. Because of that we say that this is a *gedanken experiment*, because it is not possible to perform this set up experimentally: is an ideal scenario for testing gravity beyond 4 dimensions. However, we consider that is of capital interest to study in detail the easiest scenario to perform more complicated experiments in the future.

Still, with some imagination, this set up could be used to study matter distributions in other branes. This could be done by studying the movement of a test particle in our brane. Possible movements with deviations from what is expected in a newtonian gravity, or movements with no apparent explanation (as we could not "see" the source of the gravitational field), could be explained via this scenario, that we have exposed in this paper.

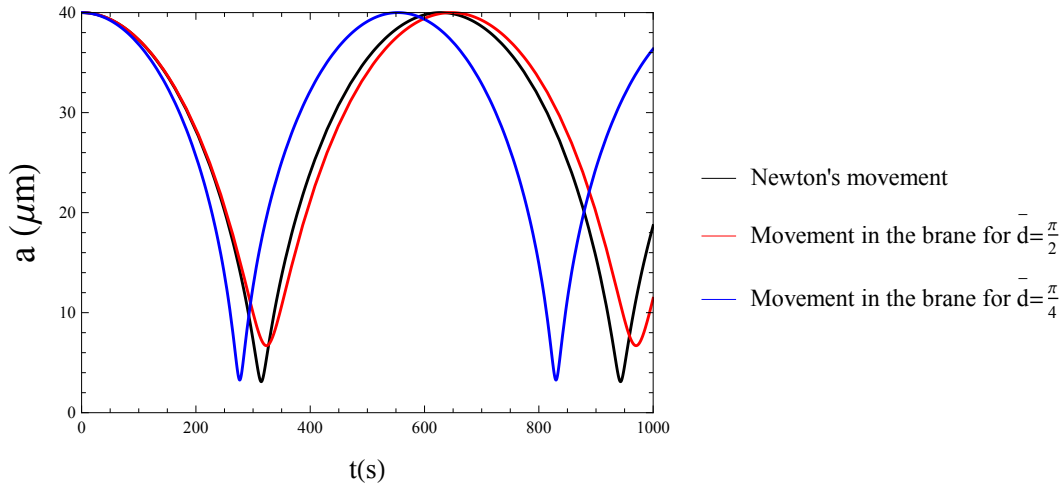


Figure 9: Orbit for a particle with initial conditions  $a = 40\mu\text{m}$ ,  $\theta = 0.0015\text{rad/s}$  and  $\dot{a} = 0$  for a newtonian movement and for two movements (for different  $d$  values) of a particle attached to a brane. We can appreciate the difference in the period of these movements and also in the minimal radius of the movements.

In Figure 9 a typical orbit for three different choices of the initial conditions is shown. This figure is useful to explain the main differences that we will look for. Some interesting things in this figure: the main one is that the period of an orbit in the brane can be larger or smaller than the newtonian one. This is in agreement with what we saw in figure 7: for smaller values of  $d$  the effective force<sup>8</sup>  $F_{BB}$  becomes stronger than Newton's square law, while for larger values of  $d$  the force becomes weaker. So, measuring the period we can, in principle, test the brane distance. We also appreciate that the minimum (or maximum) radius also changes respect to the newtonian one, and that also depends on  $d$ . This figures illustrates us that studying the period is a starting point to study the differences on the movements.

<sup>8</sup>This behaviour changes in  $\bar{d} \sim \frac{\pi}{3}$

In Figure 9 we observe that given these initial conditions the particle first approaches to the particle of mass  $M$  that is generating the potential. However, a different movement is also possible: the particle can move away to return after to the initial distance. If the initial point corresponds to  $r_{max}$  we will tell that the movement has the shape of an ellipsis with N-S orientation. In the other hand if the initial position corresponds to  $r_{min}$  we will say that the ellipsis has E-W orientation. We are also interested in finding initial conditions that lead to different ellipsis orientations for Newton's and brane movements. Experimentally deviations between both movements would be easily observed via the shape of the ellipsis.

### 3.3 Results for orbital motion

In this section we are studying if there exist appreciable differences between the orbit that a particle follows depending on what force it is suffering: if a newton square law or a force along the brane. We are going to compute three different quantities: minimal and maximal distances from the center of mass and the period of the orbit. These three quantities are those that define the orbit itself. We will compare these quantities for both forces. In particular we are going to study two different quantities. The quotient of the periods, i.e.  $Q_T = T_N/T_L$ , where  $T_N$  is the period on a newtonian orbit and  $T_L$  is the period on a 5-dimensional force orbit. The second one is the eccentricity in both movements. The eccentricity is defined as  $e = r_{max}/r_{min}$ . We will also study the orientation of the ellipsis, as we will see afterwards in more detail. As we have seen, both newton and brane forces are equal at distances five times larger than the compactification radius we expect that the orbits have appreciable differences at distances inferior to  $50\mu\text{m}$  (remember that we study the case with  $R = 10\mu\text{m}$ ).

Hereafter, we proceed to study the period and eccentricity for these movements.

#### 3.3.1 Period

Here we will study how the period changes for different initial conditions. In a newtonian movement just two initial conditions we can select: initial position<sup>9</sup> and initial velocity. For a brane-to-brane movement we also can select the distance between the two branes. As we are going to consider initial radial velocity to be zero,  $\dot{a} = 0$ , the two initial conditions will be initial radial position and initial angular velocity. In figure 10 the period for a newtonian movement is shown. This periods have been computed numerically using equation 43. We will call to the parameter space  $r - \dot{\theta}$  plane. This figure is the starting point of this subsection.

Once we have seen how the period changes for a newtonian movement, we study the comparison between two movements. Firstly we study the ratio of the periods for a fixed value of  $\dot{\theta}$ , see figure 11. We can appreciate that for distances smaller than 5 times the compactification radius there exist a considerable difference between the period of both movements. Periods at larger distances differ less than a 5 %. We also observe that for smaller values of  $\bar{d}$  the period of the brane movement becomes greater than the newtonian period. This is in good agreement with what we saw in 7, that for distances  $R < a < 4R$  the brane force is stronger than Newton's force if  $\bar{d}$  decreases. We also observe that for distances smaller than the compactification radius the period on a brane-to-brane movement becomes greater than newtonian period. This is caused because at small distances brane-to-brane force tends to zero and makes the particle orbit really slow.

In figures 12-14 the plot in the  $(a(0), \dot{\theta}(0))$  plane shows the ratio of the periods  $Q_T = T_N/T_{BB}$  for different values of  $d$  ( $\bar{d} = \pi$ ,  $\bar{d} = \pi/2$  and  $\bar{d} = \pi/4$ , respectively). In each figure we show the contours corresponding to a difference between  $T_N$  and  $T_{BB}$  greater than 20%, 10%, 5% and 1%, where darkest zones represent a more different movement. Again the dark region in the upper right side represents the

<sup>9</sup>Without loss of generality we will select  $\theta(t=0) = 0$ .

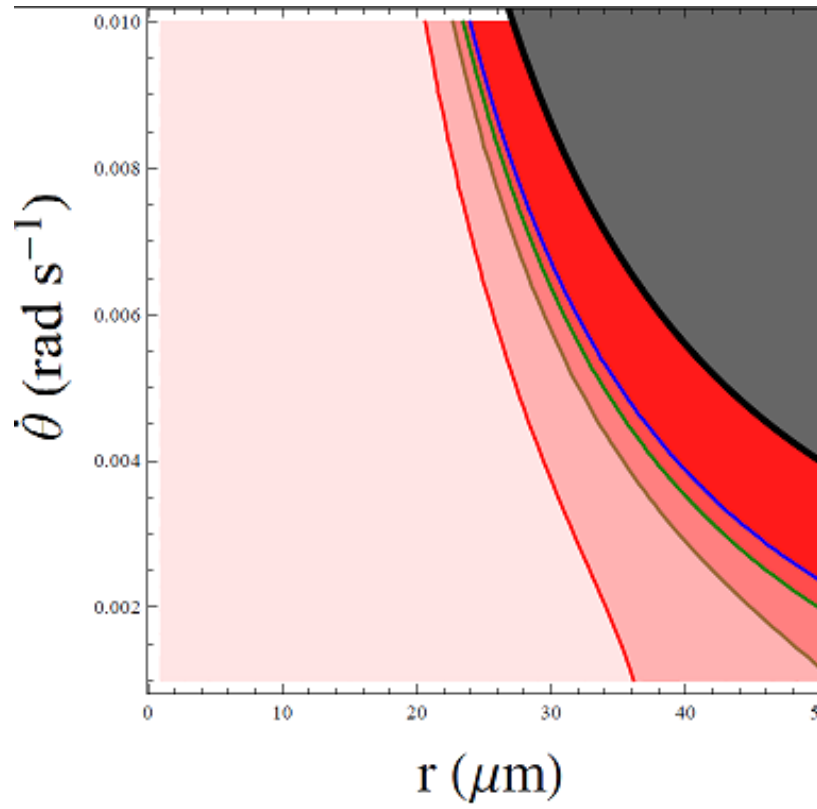


Figure 10: *Period of the orbit for a newtonian movement in the  $r - \dot{\theta}$  plane. The grey region in the right upper side corresponds to the region in which the movement is not periodic, i.e. in which the particle escapes. In the figure the darker color indicates longer periods, while lighter colors indicate shorter. The lines correspond (starting from the right side) to periods of 1500, 1200, 900 and 500 seconds.*

initial conditions that generate a non-bounded movement.

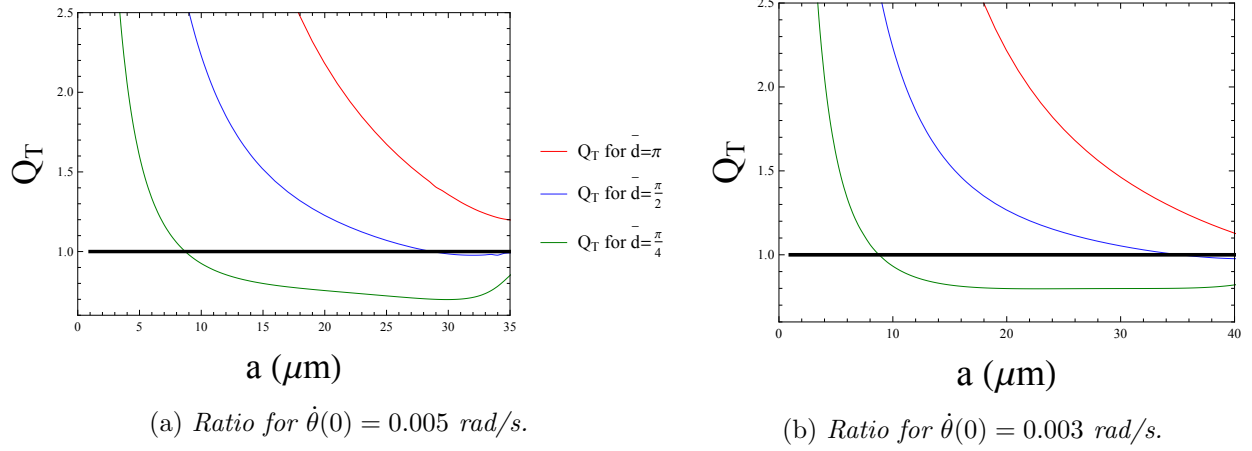


Figure 11: Ratio of the periods, for a fixed value  $\dot{\theta}$  of the movement considering brane-to-brane model and newtonian movement for different positions of the brane. Notice that the ratio tends to one, and for distances  $a \sim 5R = 50\mu\text{m}$  movements are practically equal.

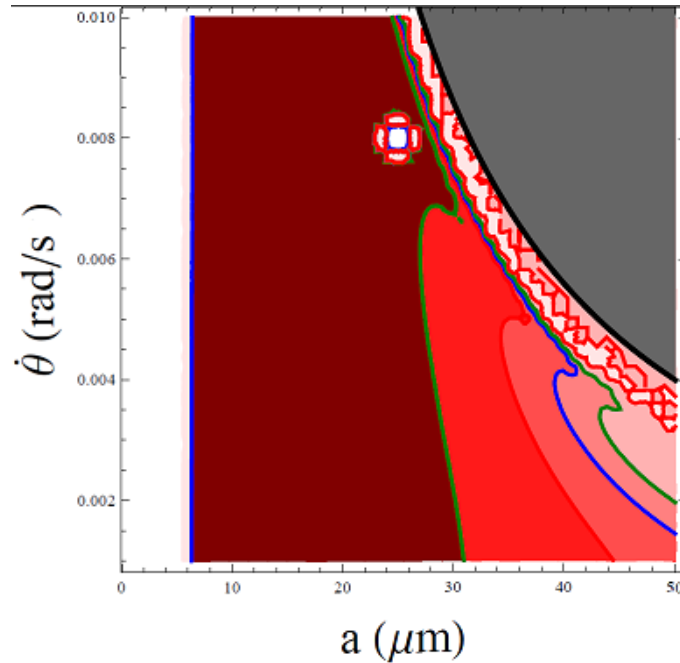


Figure 12: Ratio of the periods of the movement considering a brane model and newtonian movement for  $\bar{d} = \pi$ . The grey region in the right upper side corresponds to the region in which the movement is not periodic. Lighter zones represent the zones in which the ratio approaches to one. Darkest zone represent differences of more than a 20 % in both periods.

Figure 12 does not show any interesting region for looking deviations to Newton's law. We find what we expected: at big distances both movements are equal and they start to differ when we decrease the distance. Just at really small distances we perceive differences. We are interested in finding differences at larger radius because of the difficulty of measuring gravity at small distances. At distances grater than 5 times the compactification radius differences on both periods are inferior to 5 % for every value of angular velocity.

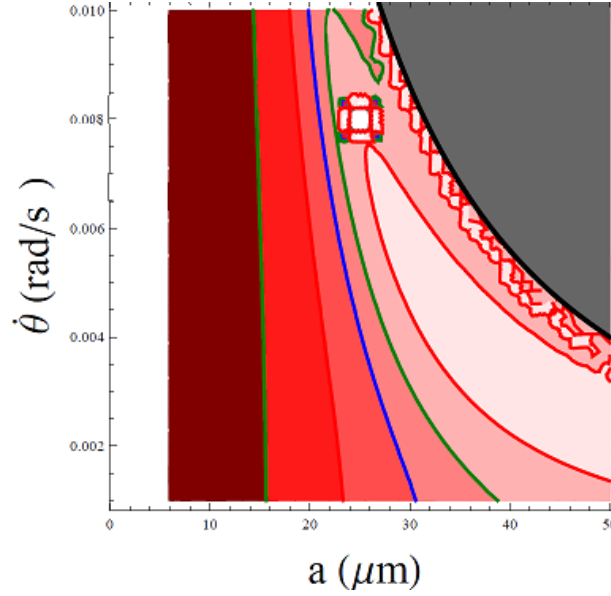


Figure 13: Ratio of the periods of the movement considering a brane model and newtonian movement for  $\bar{d} = \frac{\pi}{2}$ . The grey region in the right upper side corresponds to the region in which the movement is not periodic. Lighter zones represent the zones in which the ratio approaches to one. Darkest zone represent differences of more than a 20 % in both periods.

In figure 13 we found the same than in the previous figure but, moreover, we find that there is a region with small angular velocity where differences on the period became larger for the same radius. However, this difference is really small.

Finally, in figure 14, we find a more interesting region: there is a zone with a 20 % of difference in the periods of both movements at larger distances. We appreciate that for lower values of the angular velocity the differences become more important.

What we have learnt in these figures is that for lower distances between the two branes, differences became relevant at larger distances. We conclude this section finding that experiments should be done with lower initial angular velocities for finding easily, at larger radius, differences between brane-to-brane and newtonian movement.

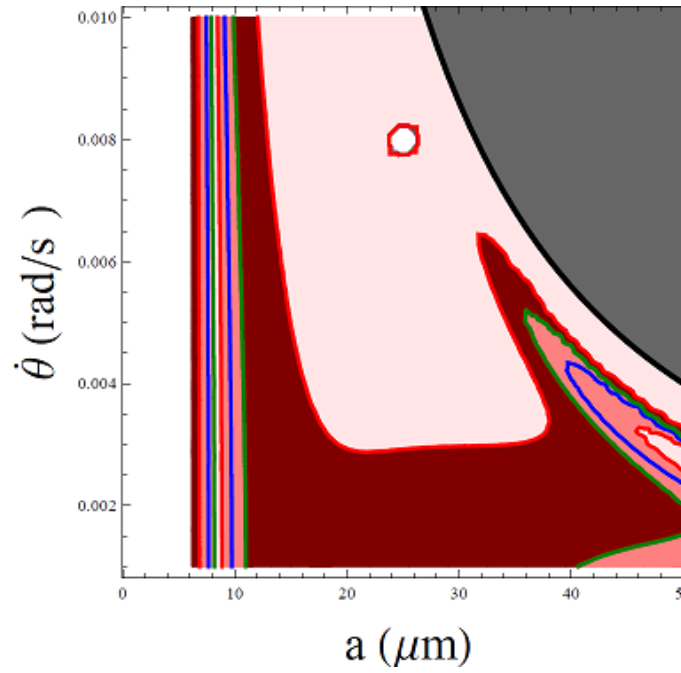


Figure 14: Ratio of the periods of the movement considering a brane model and newtonian movement for  $\bar{d} = \frac{\pi}{4}$ . The grey region in the right upper side corresponds to the region in which the movement is not periodic. Lighter zones represent the zones in which the ratio approaches to one. Darkest zone represents differences of more than a 20 % in both periods.

### 3.3.2 Eccentricity

In this section the eccentricity of the orbit is going to be studied. We are looking for a region in where eccentricity of both movements is relevant. First we see in figure 15 the shape that has the eccentricity. The black zone in the center of the figure represents the are where the orbit is circular. Darker zones represent more elliptical orbits. The darkest corresponds to a orbits with  $r_{max} > 5r_{min}$ , the next zone orbits with  $> 5\frac{r_{max}}{r_{min}} > 2$  and the central one  $2 > \frac{1}{\epsilon} > 1$ . Comparing the two subfigures we appreciate than deviations start to appear at distances smaller than  $40 \mu\text{m}$ .

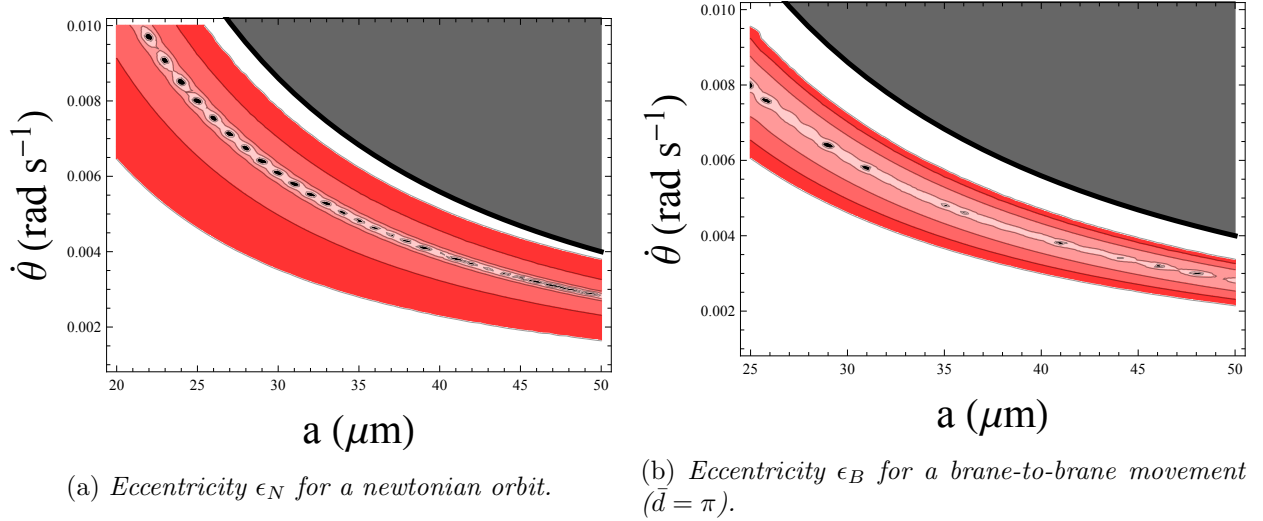


Figure 15: Eccentricity ( $\epsilon = \frac{r_{min}}{r_{max}}$ ) of the orbit of a particle suffering (a) Newton's square law, and (b) suffering effective brane-to-brane force. Darker colors show regions with major eccentricity. The central black line is when the orbit is a circle. The zones colored are beginning from the center:  $0.8 < \epsilon < 0.9$ ,  $0.5 < \epsilon < 0.8$  and  $0.2 < \epsilon < 0.5$ . The gray zone in the right upper side represents the zone where the movement is not bounded.

As we did in the previous section, we proceed to compare both movements. In particular we are going to study how varies the ratio defined by  $Q_\epsilon = \frac{\epsilon_N}{\epsilon_B}$ . In figures 16 and 17 this ratio is plotted for two different distances between the branes.

In figure 16 some comments must be done in detail. Take into account that, for larger distances, the lighter zone becomes wider, i.e. for larger distances both movements tend to have the same eccentricity. This is what we have seen during all the work: at big distances both movements are equal, and follow the expected classically. We also see that for lower values of the initial orbital velocity, the difference between both movements becomes greater. This also happened with the period, so we are obtaining compatible results: at lower values of the orbital velocity both movements are more different. A last comment must be done. When we arrive at the region  $a < 2R$  the eccentricity of the brane-to-brane movement becomes really high, leading to really big differences between to movements. As we said in the previous section, at distances inferior to the compactification radius, the brane-to-brane becomes zero, giving place to a slow and really eccentric movement.

In figure 17 is equivalent to the previous one, but we find that the differences become relevant at smaller distances. The position of the brane also plays an important role in eccentricity, so measuring this observable could be a good way of measuring  $d$ .

As we saw studying the period of the orbits, in this section, we have seen that, for lower values of the initial orbital velocity, the distances where we find more differences between the two movements, become

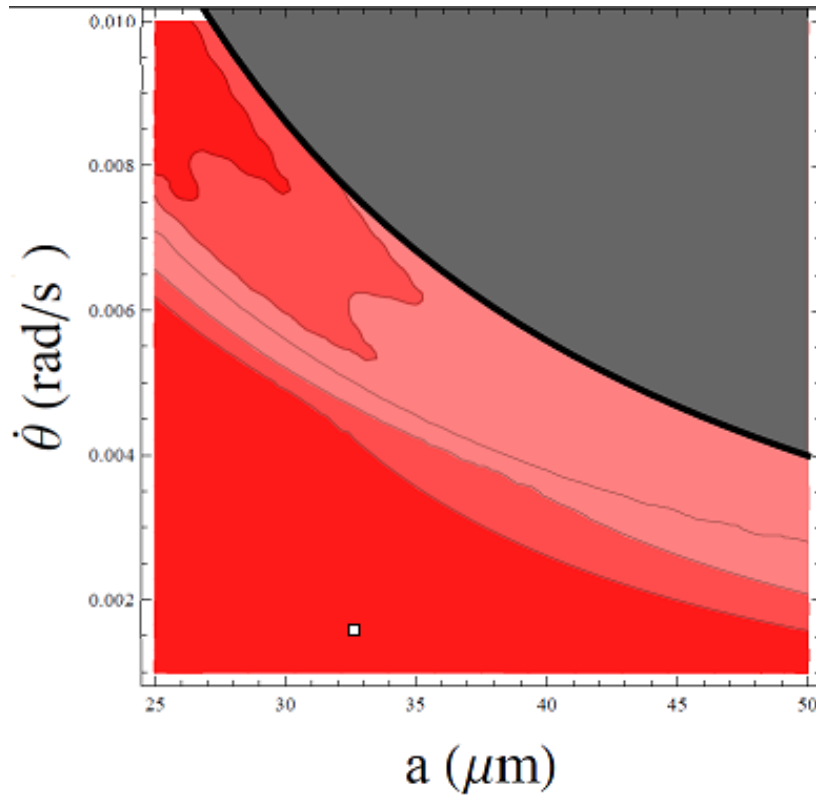


Figure 16: Ratio of the eccentricities  $Q_\epsilon = \frac{\epsilon_N}{\epsilon_B}$  for a distance between the branes  $\bar{d} = \pi$ . The grey zone in the upper right side indicates the zone when the movement is not bounded. Darker color represents the zone where  $Q_\epsilon$  differs more from the unit, i.e the zones where both eccentricities are more different. Darkest zone is the one where two eccentricities differ in a factor two or more, while lightest zone represent a difference inferior to 5 %.

grater, i.e. lowering the initial angular velocity we can develop experiments with major accuracy. This is due to that the major difficulty in measuring gravity is that for short distances Van der Waals forces become to strong and spoil the experiment.



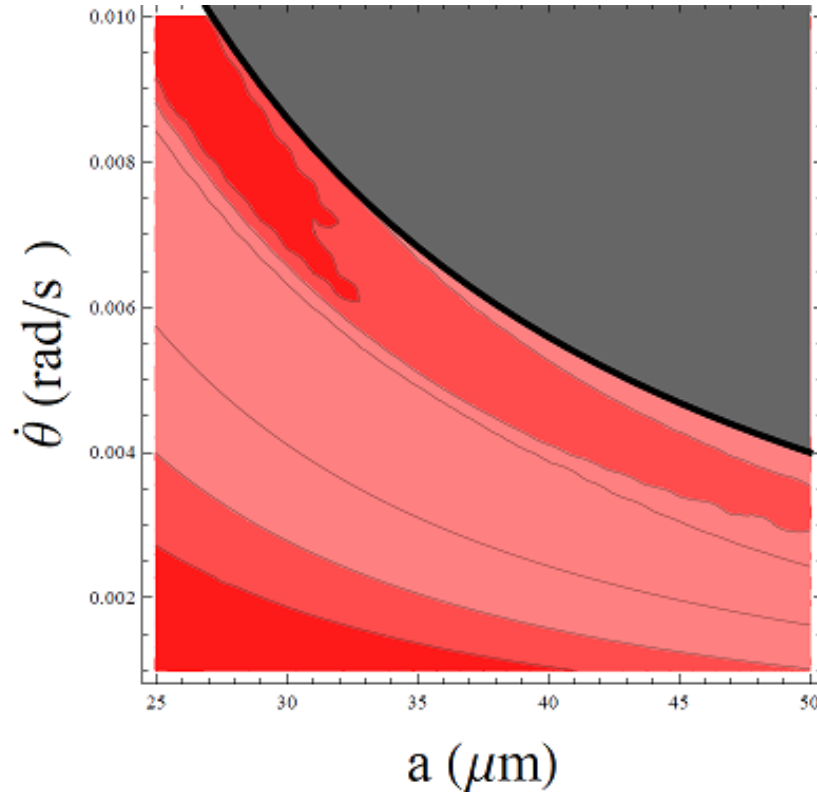


Figure 17: Ratio of the eccentricities  $Q_\epsilon = \frac{\epsilon_N}{\epsilon_B}$  for a distance between the branes  $\bar{d} = \pi$ . The grey zone in the upper right side indicates the zone when the movement is not bounded. Darker color represents the zone where  $Q_\epsilon$  differs more from the unit, i.e the zones where both eccentricities are more different. Darkest zone is the one where two eccentricities differ in a factor two or more, while lightest zone represent a difference inferior to 5 %.

## 4 Overview and open problems when facing DM

In this last section we will expose the open problems that must be studied in more detail in this scenario. There is plenty of cosmological data that has to be compared with the scenario proposed in this work. In section 4.1 we review the CMB; in section 4.2 and 4.3 we introduce DM searches, via direct and indirect observation, respectively; and at last we introduce BAO and rotational curves in sections 4.4 and 4.5, respectively. Notice that each of these subjects could be the starting point of a PhD thesis on its own, and we hope to develop them in the future.

### 4.1 Cosmic Microwave Background (CMB)

The early Universe was composed of electrons, baryons and photons that formed a really hot and dense plasma. Photons were trapped because of Thompson scattering, that made them to interact via electromagnetism with electrons and baryons. As the universe expanded, the plasma cooled and then, the combinations of baryons and electrons forming hydrogen was possible, This is known as recombination and happened at a redshift  $z \sim 1000$  (400000 years ago). After recombination, photons interacted a lot less with hydrogen atoms and they were able to travel freely. Then, the Universe became transparent to radiation. These photons that escape of the plasma at recombination time have travelled across the Universe and arrive to every part of the Universe, with no discernible source, nowadays. These photons are known as Cosmic Microwave Background (CMB) as they are microwaves of  $\sim 2.7K$ . Observing this radiation we are able to see how was the Universe after recombination time. The most accurate measurements at the CMB at present are those given by the PLANCK experiment [24].

We do not expect that our model introduces nothing new in what CMB refers. Our scenario is similar in some aspects to those proposed in mirror matter scenarios (see for example [25]), where it is shown that the CMB data can be reproduced with no particular assumptions.

### 4.2 Direct observation

Direct observation of DM particles consists on measuring a non-gravitational interaction between DM particles and ordinary SM particles. CDM models use commonly Weakly Interacting Massive Particles (WIMPs) as a possible candidate to form DM [26]. WIMPs are expected to have a mass quite larger than neutrinos. These WIMPs interact via weak interaction (or some other unknown "weak" interaction) with ordinary matter. Models predict that WIMPs have been produced very early in the history of the Universe. However, they have a really small cross-section of interaction with ordinary matter so they have hardly interacted during the Universe expansion. Because of the smallness of the cross-section detectors with large mass must be constructed.

Different experiments have been proposed for measuring this collisions, via nuclear recoil, see for example [27], that is being implemented in NEXT experiment (see for example [28]). A wind of WIMPs, of velocity around 230 km/h, with a determined directionality is expected, as this particles have travelled since Big Bang. Some experiments (DAMA, LIBRA and GOGENT<sup>10</sup>) look for this wind of winds measuring nuclear recoil during long periods of time. Because of the movement of the earth, an annual period of these interactions is expected. More interactions should happen when we are travelling in the opposite direction to the wind than when we are travelling in the same direction. This method also gives us the directionality of the WIMPs. Other experiment looking for direct observation is CDMS (Cryogenic Dark Matter Search) in which a cold material is used generating that the atoms vibrate really slow. If a WIMP

<sup>10</sup>This experiments have some data that shows that this wind has been found. However other experiments that proceed in the same way have not found it, so it is thought that this experiments are wrong.

interact with this atoms a sound wave would be generated.

In this model direct observation is not possible. As we have said, only gravitational interaction with other branes is possible, so the unique form to detect DM is indirectly or via gravitation, as we expose in the next section.

### 4.3 Indirect Observation

Indirect observations consist on detecting particles generated by the annihilation of a DM particle and his antiparticle. In indirect searches of DM WIMPs the assumption is that (if WIMPs density is enough) two WIMPs collide and they produce two SM particles via an unknown cross-section  $\sigma_{DM}$  to be measured. If the SM particles produced are weakly interacting as neutrinos, they can travel from the source and be detected, for example, in Super-Kamiokande (see figure 18). Non-observation puts bounds on  $\sigma_{DM}$  and on the WIMPs masses. Looking to the Sun (or the galactic centre), that is very heavy and should have more WIMPs nearby, has been proposed. In our case, DM annihilation is expected to produce KK gravitons that couple also to SM matter. Because DM in our model is formed of SM-like particles, the processes that we look for are of the type: matter antimatter annihilation producing KK gravitons, in the other brane, and afterwards the interaction of the graviton with matter in our brane. Some examples are shown in the figure 19.

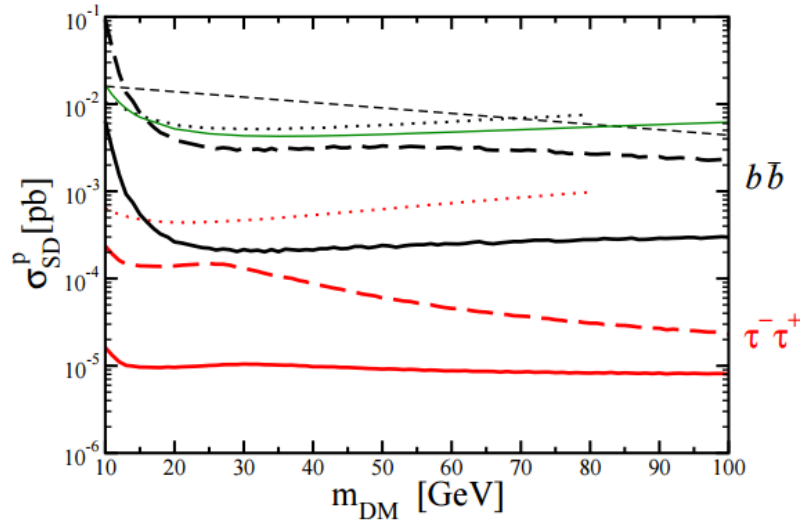
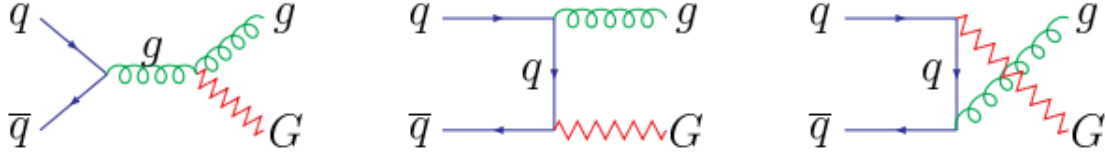


Figure 18: Figure extracted from [29], data used from DeepCore (IceCube) . In it we can see the cross-section as a function on the mass of the WIMP for different processes. Black (upper) lines refer to annihilations into  $b\bar{b}$  and red (lower) lines to annihilations into  $\tau^-\tau^+$ .

For measuring gravitons, firstly, we have to know how they interact with ordinary matter. In [30] gravitons propagation, due to interaction with SM fields, along the extra dimensions has been explicitly developed. This is a  $4+n$  dimensional theory that compactifies through a KK reduction (see Appendix B) in a  $3+1$  dimensional effective theory valid at energies below  $M_D$ .

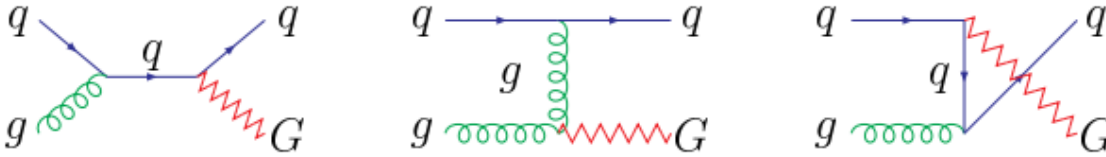
After the production of the gravitons they have to travel across the extra dimensions and interact with matter in our brane. So two different ways of observing these processes are possible: the first one is observing the collision of gravitons with SM particles (it can be measured by nuclear recoil for example), whereas that the second one is observing processes with violation of energy, energy that has the graviton that escapes from the brane, see figure 20.

•  $q\bar{q} \rightarrow gG$



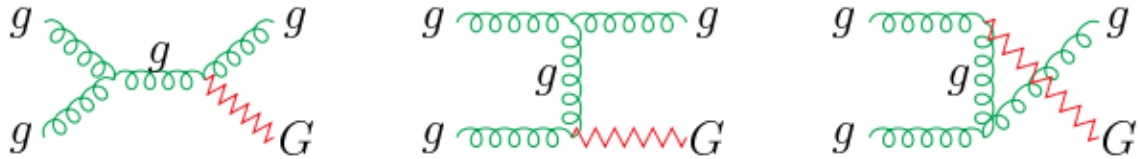
(a) Quark and antiquark annihilation producing a gluon and a graviton.

•  $qg \rightarrow qG$



(b) Quark and gluon interaction producing a quark and a graviton.

•  $gg \rightarrow gG$



(c) Two gluons producing a gluon and a graviton.

Figure 19: Different ways of producing gravitons by collisions  $p\bar{p}$  [31]. These Feynman diagrams are based in a low-energy effective theory and they are only valid for energies inferior to the scale  $M_D$ . For a review on the actual experimental bound see for example [32]

#### 4.4 Baryonic Acoustic Oscillations (BAO)

The early Universe had homogeneous density anisotropies of 10 parts per million. However, when we observe the Universe today we find large structure and density fluctuations. These fluctuations, known as BAO, are regular and periodic. The current belief is that small anisotropies acted as gravitational seeds for the structure we see today, i.e. the denser parts of the Universe attracted more matter, giving place to galaxies, clusters and superclusters, while the less dense parts became vacuum. Thus, these small anisotropies we see in the CMB lead to the large scale structures we observe in the universe today. BAO measurements have also helped to understand more about the nature of dark energy.

Nowadays, plenty of simulations are being done for testing DM models. Depending on the quantity or the initial distribution of dark energy, baryonic matter and dark matter the evolution of the Universe changes. These simulations are done for finding models that fit CMB observations. Simulations of structure formation in the presence of two or more branes must be done in the future to test the validity of this scenario.

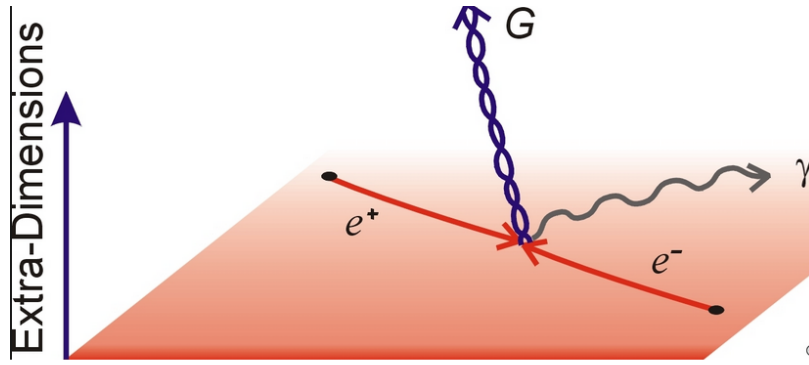


Figure 20: This imagine shows a possible way of detecting the existence of extra dimensions. Annihilation on a pair  $e^+e^-$  produces a photon and a graviton that escapes from the brane carrying energy.

A possibility also proposed is the existence of a non-trivial field profile (see for example <sup>11</sup> [33]). Different copies of SM would happen in each brane (different couplings, masses...). This generates an asymmetry between branes and they will evolve in different ways. This could generates also explanations why DM is dissipationless in some branes. Small changes in coupling and masses could generate drastic changes in structure formation.

#### 4.5 Rotational curves and gravitational lensing

Rotational curves refer to the measurement of the orbital velocity of stars around the galaxy. Gravitational lensing is produced by the deviation, caused by the curvature of the space generated by massive objects, of the photons when they travel long distances. Gravitational lensing allows us to compute the mass distribution of galactic objects via the study of the light that comes from behind them. Due to data produced by rotational curves and gravitational lensing a particular distribution of DM is expected: forming a big halo that involves the galaxy (see figure 21). This halo make us think that DM is non-dissipating.

The main problem in our scenario is that baryonic matter dissipates while CDM models predict non dissipating DM. The dissipational processes are responsible for the formation of condensed structures. Astrophysical observations show that DM forms only galactic halos, and not smaller objects (at least the major part of it). If we have two parallel branes with the same initial density DM should be as dissipating as baryonic matter and also be the same amount of DM and baryonic matter ( $\Sigma_B = \Sigma_{DM}$ ). Furthermore small structures should be formed of DM: galaxies, stars or even planets. Moreover hybrid structures of DM and baryonic matter should be formed, structures that have never been observed.

However, the solution is to suppose the existence of many parallel branes and that the density in these branes is smaller than in our brane. If the density is smaller dissipation is also small. This assumption would imply that DM is dissipating but that there has been not enough time to form small structures. If the density is 4 times smaller in the brane galaxies formation would be starting now.

<sup>11</sup>In this paper a brane folded many times is considered. The folding generates many parallel 4-branes. Matter in parallel branes only interact gravitationally so it is a possible explanation for Dark Matter (DM).

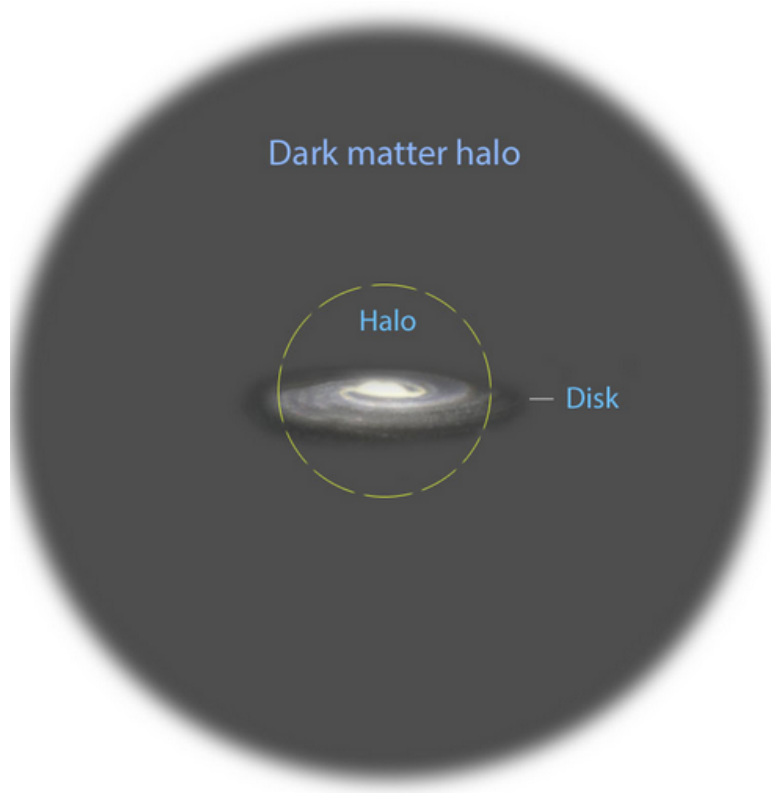


Figure 21: *Representation of the DM halo that involves the galaxy.*

## 5 Conclusions

In this work we have studied a 5-dimensional scenario with the presence of two branes looking for a DM candidate. Our explanation is that DM is nothing but SM matter placed in other brane. Because SM fields are attached to the branes, we only interact via gravitation with the other brane and we do not see this matter. Introducing a compactified dimension also helped us to decrease considerably gravity scale.

In section 2 the potential and the force that particles suffer in this scenario were computed. The brane make the particle move along it, it produced the same effect than an inclined plane. We saw that for distances larger compared with the compactification radius the force felt by a particle in 5 dimensions was Newton's square law, reproducing experimental data. We have to go to distances of the order of the compactification radius for finding deviation to Newton's law. The experimental bounds were exposed and the deviations were parametrized using a Yukawa type potential. In this section we saw at what distances we could test gravity, selecting our  $R$  value.

Afterwards, in section 3, we studied a *gedanken experiment*. The experiment consisted in placing just one particle in each brane and study if this ideal scenario had differences with newtonian one. A lot of efforts were done trying to make possible this *gedanken experiment*, but we concluded that we do not have enough technology for achieving it.

We computed some observables like the period of the orbits and the eccentricity. We concluded that for lower values of the initial angular velocity the distances where appear discernible differences between the movements became larger. This helped because testing gravity at distances inferior to  $100 \mu\text{m}$  is really difficult. Nevertheless we concluded that distance in where deviations become relevant are those where  $a < 5R$ .

As we have seen in section 4 a lot of work remains to be done. Models for understanding how we detect indirectly DM must be studied in detail. Also simulations for testing BAO data. The most challenging point are those referring to rotational curves and gravitational lensing, but we expect that with the existence of many less dense branes the problem of the dissipation of DM and the formation of the big galactic halo is solved.

Perhaps this model does not bring any discovery to physics, and it could be considered a funny idea in a few years, when DM will be eventually understood. Still, we hope that our work and what will follow would be useful and represents a small step forward, or at least not backwards, in the fight revealing the secrets of the Universe.

## 6 Appendix A: Conventions

In this appendix we expose the conventions that we follow during the work.

When we talk about 4-branes we are considering objects with 3 spatial dimensions and one temporal dimension. The temporal dimension is the same for all branes.  $n$  is the number of extra dimensions,  $D$  is the total number of dimensions, so  $D = n + 4$ . The position in our brane is:  $\vec{x} = (x_1, x_2, x_3)$ , while the direction in the extra dimension is  $\vec{y} = (y_1, y_2, y_3, \dots, y_n)$ . The position vector is so  $r = \sqrt{\vec{x}_i^2 + \vec{y}_n^2}$ . We often will call  $a^2 = x_1, x_2, x_3$ , this distance also will be called as distance in the brane, and  $\vec{a}$  will be called brane direction, as it has no component in the extra dimension. We would always use  $r$  as the distance between two bodies.  $d$  is the distance between the two branes being  $\bar{d} = \frac{d}{R}$ . In the classical scenario, where we only have three spatial dimensions, we will use indistinctly  $a$  and  $r$  for the radial distance, if there is not possibility of confusion.

Latin index (i,j,k..) run from 1 to 3, while Greek index run from 0 to 3 (0 represents time) and we use capital Latin letters for index that run from 0 to  $D$ . The metric is a  $n \times n$  matrix, in the case of  $n = 1$  we have :

$$x^\mu = (x^0, x^1, x^2, x^3) = (t, x^1, x^2, x^3), x^A = (x^0, x^1, x^2, x^3, y^1, \dots, y^n) \text{ for } d = 1$$

$$x^A = (x^0, x^1, x^2, x^3, y)$$

$$g_{MN} = \begin{pmatrix} 1 & 0 & 0 & 0 & 0 \\ 0 & -1 & 0 & 0 & 0 \\ 0 & 0 & -1 & 0 & 0 \\ 0 & 0 & 0 & -1 & 0 \\ 0 & 0 & 0 & 0 & -1 \end{pmatrix}. \quad (46)$$

We are going to use mainly to forces during this work. We refer to Newton's square law to the habitual classical force. We call brane force to the force resulting of the presence of extra dimensions and the brane. This force is similar at the one of an inclined plane, it is an effective force that not goes in the radial direction that unites both particles. The force that unites both particles is called 5-dimensional force and it is not of particular interest in this work.

We will call to the distance between the two branes  $d$ , and  $\bar{d} = \frac{d}{R}$  is this distance normalized to the compactification radius. The distance along the brane is  $a$ , and  $\bar{a} = \frac{a}{R}$  is the distance normalized to the compactification radius. This distance is used because its simplicity for computing corrections at large and small distances.

## 7 Appendix B: Kaluza and Klein hypothesis (KK)

This was the first proposal with more than three spatial dimensions. It was introduced in the 20s, regardless, by the physicians Kaluza and Klein. They intended to unify all the forces known in their time, i.e. gravity and electromagnetism. In this section we will solve the motion equation of a free scalar particle in 5 dimensions, as Kaluza and Klein did, and afterwards in section 3, with the method learned in this section, we will be able to study the gravitational potential generated by a massive particle in 5 dimensions. We will also study their limit and short and big distances, and we will study possible corrections to Newton's gravitation law.

In 1921 Theodor Kaluza<sup>12</sup> [35] published for first time a theory which intended to unify gravity with electromagnetism. He realized a generalization of Einstein's relativity considering a space-time with an

<sup>12</sup>For a compilation of the original text see for example [34].



extra spatial compactified dimension<sup>13</sup>. Kaluza's idea was to consider each geodesic as a cylinder. This cylinder is not observable because of the small of the extra dimension. He tried to explain electromagnetic field through the curvature of the extra dimension.

In 1926 Oskar Klein [36] introduced quantum mechanics in Kaluza's theory. Imposed quantization of the momentum in the extra dimension (for being finite the space not all the momentums are possible). He found that the size of the extra dimension was too small,  $r_5 \sim 10^{-30}cm$ , and for that reason unobservable.

We are going to reproduce the results that Kaluza and Klein obtained. We are going to solve the motion equation for a free particle in 5 dimensions. Results can be extended for spaces with more than 5 dimensions. For the conventions see Appendix A. The Lagrangian of a free scalar particle can be written as:

$$\mathcal{L} = \frac{1}{2}g^{MN}\partial_M\Phi(x,y)\partial_N\Phi(x,y) - \frac{M^2}{2}\Phi(x,y) = \frac{1}{2}\partial^N\Phi(x,y)\partial_N\Phi(x,y) - \frac{M^2}{2}\Phi(x,y) , \quad (47)$$

that is the habitual Lagrangian for a free massive particle with mass  $M$  but adding one more dimension. Applying Euler-Lagrange equations we obtain the following motion equation:

$$\square_5\Phi(x,y) + M^2\Phi(x,y) = 0 , \quad (48)$$

where  $\square_5$  is the d'Alembertian with one more dimension. It satisfies the relation  $\square_5 = \square_4 - \frac{d^2}{dy^2}$ , with  $\square_4 = \partial^\mu\partial_\mu$ . We are going to look for a solution using separation of variables method. We are supposing a factorizable metric, i.e.  $\mathcal{M}_5 = \mathcal{M}_4 \otimes S_1$ , where  $\mathcal{M}_4$  is Minkowski metric and  $S_1$  is just a circle. We expect that this is true because we do not have any experimental evidence of the extra dimension, i.e. we expect that this dimension is separable from the other 4. We then can write  $\Phi(x,y) = \phi(x)\psi(y)$  and we obtain:

$$[\square_4\phi(x)]\psi(y) + \phi(x)[\square_4\psi(y)] - \frac{d^2\phi(x)}{dy^2}\psi(y) - \phi(x)\frac{d^2\psi(y)}{dy^2} + M^2\phi(x)\psi(y) = 0 , \quad (49)$$

where second and third terms are zero. We can write:

$$\frac{\square_4\phi(x)}{\phi(x)} = \frac{\frac{d^2\psi(y)}{dy^2} + M^2}{\psi(y)} = -k^2 . \quad (50)$$

The left side depends only on  $x$  and the right side only depends on  $y$  so both must be equal and constant, denoted by  $-k^2$  for convenience. We have to solve the following equations:

$$\begin{cases} \square_4\phi(x) + k^2\phi(x) = 0 \\ \frac{d^2\psi(y)}{dy^2} + [k^2 - M^2]\psi(y) = 0 \end{cases} . \quad (51)$$

The solution to the first equation are plane waves  $\phi(x) = e^{\pm ikx}$ , the habitual solution for a free particle, and second equation is the normal harmonic oscillator, with familiar solution  $\psi(y) = Ae^{-i\omega y} + Be^{i\omega y} = C\cos(\omega y) + D\sin(\omega y)$ , with  $\omega = \sqrt{k^2 - M^2}$ . We now have to impose periodic conditions in the fifth dimension, i.e.  $\psi(y) = \psi(y + 2\pi R)$ . With this we are introducing the compactification. We obtain:

$$C\cos(\omega y) + D\sin(\omega y) = C\cos[\omega(y + 2\pi R)] + D\sin[\omega(y + 2\pi R)] , \quad (52)$$

<sup>13</sup>When we talk about a compactified dimension we are referring to a finite size and periodic dimension. A normal dimension is infinite and not periodic.

with  $R$  being the compactification radius of the extra dimension. This is only true if  $\omega R = n$ , with  $n$  an integer.  $k$  can be related with the particle's quadrimomentum,  $k = (E, \vec{k})$ , while  $\omega$  represents the momentum in the fifth dimension  $k^2 = E^2 - |\vec{k}|^2 = M^2 + \omega_n^2$ . We can write then  $E_n^2 = M^2 + |\vec{k}|^2 + \omega_n^2$ , that is the dispersion relation in five dimensions.

We know that a scalar field can be quantized as follows:

$$\Phi(x) = \sum_k \left[ a(\vec{k}) e^{-ikx} + a^\dagger(\vec{k}) e^{ikx} \right], \quad (53)$$

where  $a(\vec{k})$  and  $a^\dagger(\vec{k})$  are the common creation and destruction operators and, if  $k$  varies continuously,  $\sum_k \sim \int \frac{d^3k}{(2\pi)^3}$ . This allows us to decompose fields of theories in 4 dimensions in plane waves. If we study the field in 5 dimensions, we can express it as the one in four dimensions multiplied by a plane wave in the extra dimension, but with quantified momentum, we can develop as follows:

$$\begin{aligned} \Phi(x, y) &= \sum_{m=-\infty}^{\infty} N_m \left[ \phi_m(x) e^{\frac{-imy}{R}} + c.c. \right] = \\ &= \sum_{m=-\infty}^{\infty} N_m \left[ \phi_m(x) \left( \cos \frac{my}{R} - i \sin \frac{my}{R} \right) + c.c. \right] = \\ &= N_0 \phi_0(x) + N \sum_{m=1}^{\infty} \phi_m(x) \left( \cos \frac{my}{R} - i \sin \frac{my}{R} \right) + N \sum_{m=1}^{\infty} \phi_{-m}(x) \left( \cos \frac{my}{R} + i \sin \frac{my}{R} \right) + c.c. = \quad (54) \\ &= N_0 \phi_0(x) + N \sum_{m=1}^{\infty} \{ (\phi_m(x) + \phi_{-m}(x)) \cos \frac{my}{R} \} - iN \sum_{m=1}^{\infty} \{ (\phi_m(x) - \phi_{-m}(x)) \sin \frac{my}{R} \} = \\ &= \frac{1}{\sqrt{\pi R}} \left[ \sum_{m=0}^{\infty} \varphi_m^e(x) \cos \frac{my}{R} + \sum_{m=1}^{\infty} \varphi_m^o(x) \sin \frac{my}{R} \right], \end{aligned}$$

where we have defined even and odd fields with respect  $\phi = (0, 2\pi R)$ :

$$\begin{cases} \varphi_0^e = \frac{1}{\sqrt{2}} \phi_0 \\ \varphi_m^e(x) = \frac{1}{\sqrt{2}} (\phi_m + \phi_{-m}) \\ \varphi_m^o(x) = \frac{-i}{\sqrt{2}} (\phi_m - \phi_{-m}) \end{cases}, \quad (55)$$

with the normalization:

$$N_0^2 \int_0^{2\pi R} dx |\Phi_0(x)|^2 = 1, \quad N_0 = \frac{1}{\sqrt{2\pi R}}, \quad (56)$$

$$N^2 \int_0^{2\pi R} dx |\Phi_n(x)|^2 = 1, \quad N = \frac{1}{\sqrt{\pi R}}. \quad (57)$$

We have obtained that a theory in 5 dimensions with just one field can be decomposed into a theory 4 dimensional theory with infinite fields. This is called a Kaluza-Klein (KK) reduction and was one of the main result obtained in this model. We have a zero mode  $\phi_0(x)$ . This field represents a massless particle, with no momentum in the fifth dimension. The other fields represent an infinite tower of mass states with

$\omega_n = \frac{n}{R}$ , denoted as Kaluza-Klein tower. This states represent identical particles to the massless one but that differ in the mass. This model could be proved in this way, finding identical particles with different mass.

This section has been useful for introducing the starting point of the next section. When we consider a compactified dimension a Kaluza-Klein tower is going to appear, and we have to do a summation over it.

## References

- [1] S. L. Glashow, “Beating the standard model,” 1998.
- [2] P. W. Higgs, “Broken symmetries, massless particles and gauge fields,” *Phys.Lett.*, vol. 12, pp. 132–133, 1964.
- [3] F. Englert and R. Brout, “Broken Symmetry and the Mass of Gauge Vector Mesons,” *Phys.Rev.Lett.*, vol. 13, pp. 321–323, 1964.
- [4] G. Altarelli, “The Higgs and the Excessive Success of the Standard Model,” 2014.
- [5] M. Fukugita and T. Nakamura, “COMMENT ON THE NEUTRINO OBSERVATION FROM SN1987a IN THE KAMIOKANDE DETECTOR,” 1987.
- [6] G. Aad *et al.*, “Observation of a new particle in the search for the Standard Model Higgs boson with the ATLAS detector at the LHC,” *Phys.Lett.*, vol. B716, pp. 1–29, 2012.
- [7] S. Chatrchyan *et al.*, “Observation of a new boson at a mass of 125 GeV with the CMS experiment at the LHC,” *Phys.Lett.*, vol. B716, pp. 30–61, 2012.
- [8] G. ’t Hooft, “Naturalness, chiral symmetry, and spontaneous chiral symmetry breaking,” *NATO Adv.Study Inst.Ser.B Phys.*, vol. 59, p. 135, 1980.
- [9] S. P. Martin, “A Supersymmetry Primer,” 2011.
- [10] K. Lane, “Two lectures on technicolor,” 2002.
- [11] I. Antoniadis, S. Dimopoulos, and G. Dvali, “Millimeter range forces in superstring theories with weak scale compactification,” *Nucl.Phys.*, vol. B516, pp. 70–82, 1998.
- [12] I. Antoniadis, N. Arkani-Hamed, S. Dimopoulos, and G. Dvali, “New dimensions at a millimeter to a Fermi and superstrings at a TeV,” *Phys.Lett.*, vol. B436, pp. 257–263, 1998.
- [13] L. Randall and R. Sundrum, “A Large mass hierarchy from a small extra dimension,” *Phys.Rev.Lett.*, vol. 83, pp. 3370–3373, 1999.
- [14] L. Randall and R. Sundrum, “An Alternative to compactification,” *Phys.Rev.Lett.*, vol. 83, pp. 4690–4693, 1999.
- [15] E. Floratos and G. Leontaris, “Low scale unification, Newton’s law and extra dimensions,” *Phys.Lett.*, vol. B465, pp. 95–100, 1999.
- [16] H. Liu, “Compactified Newtonian potential and a possible explanation for dark matter,” 2003.
- [17] M. B. Green, J. Schwarz, and E. Witten, “SUPERSTRING THEORY. VOL. 1: INTRODUCTION,” *Cambridge Monogr.Math.Phys.*, 1987.
- [18] M. B. Green, J. Schwarz, and E. Witten, “SUPERSTRING THEORY. VOL. 2: LOOP AMPLITUDES, ANOMALIES AND PHENOMENOLOGY,” 1987.

- [19] J. Polchinski, “Tasi lectures on D-branes,” pp. 293–356, 1996.
- [20] J. Polchinski, S. Chaudhuri, and C. V. Johnson, “Notes on D-branes,” 1996.
- [21] N. Arkani-Hamed, S. Dimopoulos, and J. March-Russell, “Stabilization of submillimeter dimensions: The New guise of the hierarchy problem,” *Phys.Rev.*, vol. D63, p. 064020, 2001.
- [22] N. Arkani-Hamed, S. Dimopoulos, and G. Dvali, “Phenomenology, astrophysics and cosmology of theories with submillimeter dimensions and TeV scale quantum gravity,” *Phys.Rev.*, vol. D59, p. 086004, 1999.
- [23] A. Kehagias and K. Sfetsos, “Deviations from the  $1/r^{**2}$  Newton law due to extra dimensions,” *Phys.Lett.*, vol. B472, pp. 39–44, 2000.
- [24] A. Marchini and V. Salvatelli, “Updated constraints from the PLANCK experiment on modified gravity,” *Phys. Rev.*, vol. D88, no. 2, p. 027502, 2013.
- [25] Z. K. Silagadze, “TeV scale gravity, mirror universe, and ... dinosaurs,” *Acta Phys. Polon.*, vol. B32, pp. 99–128, 2001.
- [26] arXiv:0911.0323v1 [astro-ph.CO] 1 Nov 2009
- [27] D. Nygren, “Columnar recombination: a tool for nuclear recoil directional sensitivity in a xenon-based direct detection WIMP search,” *J.Phys.Conf.Ser.*, vol. 460, p. 012006, 2013.
- [28] V. Ivarez *et al.*, “Ionization and scintillation response of high-pressure xenon gas to alpha particles,” *JINST*, vol. 8, p. P05025, 2013.
- [29] C. R. Das, O. Mena, S. Palomares-Ruiz, and S. Pascoli, “Determining the Dark Matter Mass with DeepCore,” *Phys. Lett.*, vol. B725, pp. 297–301, 2013.
- [30] G. F. Giudice, R. Rattazzi, and J. D. Wells, “Quantum gravity and extra dimensions at high-energy colliders,” *Nucl.Phys.*, vol. B544, pp. 3–38, 1999.
- [31] D. Acosta *et al.*, “Search for Kaluza-Klein graviton emission in  $p\bar{p}$  collisions at  $\sqrt{s} = 1.8$ -TeV using the missing energy signature,” *Phys.Rev.Lett.*, vol. 92, p. 121802, 2004.
- [32] H. Sun, “Large Extra Dimension effects through Light-by-Light Scattering at the CERN LHC,” *Eur.Phys.J.*, vol. C74, p. 2977, 2014.
- [33] N. Arkani-Hamed, S. Dimopoulos, G. Dvali, and N. Kaloper, “Many fold universe,” *JHEP*, vol. 0012, p. 010, 2000.
- [34] S. Wesson, “Modern Kaluza-Klein Theories,” 1999.
- [35] T. Kaluza, “Zum Unittsproblem in der Physik Sitzungsber.,” *Preuss*, vol. Akad, 1921.
- [36] O. Klein, “Quantentheorie und fnfdimensionale Relativittstheorie Zeitschrift fr Physik,” *Preuss*, vol. Akad, pp. 895–906, 1926.